

Linear Optimal Transport Embedding: Provable fast Wasserstein distance computation and classification for nonlinear problems

Caroline Moosmüller* Alexander Cloninger*[†]

Abstract

Discriminating between distributions is an important problem in a number of scientific fields. This motivated the introduction of Linear Optimal Transportation (LOT), which embeds the space of distributions into an L^2 -space. The transform is defined by computing the optimal transport of each distribution to a fixed reference distribution, and has a number of benefits when it comes to speed of computation and to determining classification boundaries. In this paper, we characterize a number of settings in which LOT embeds families of distributions into a space in which they are linearly separable. This is true in arbitrary dimension, and for families of distributions generated through perturbations of shifts and scalings of a fixed distribution. We also prove conditions under which the L^2 distance of the LOT embedding between two distributions in arbitrary dimension is nearly isometric to Wasserstein-2 distance between those distributions. This is of significant computational benefit, as one must only compute N optimal transport maps to define the N^2 pairwise distances between N distributions. We demonstrate the benefits of LOT on a number of distribution classification problems.

1 Introduction

The problem of supervised learning is most commonly formulated as follows. Given data of the form $\{(x_i, y_i)\}_{i=1}^N$ where $x_i \in \mathbb{R}^n$, learn a function $f : \mathbb{R}^n \rightarrow \mathbb{R}$ such that $f(x_i) \approx y_i$. However, in many applications the data points are not simply points in \mathbb{R}^n , but are instead probability measures μ_i on \mathbb{R}^n , or even finite samples $X_i = \{x_j^{(i)}\}_{j=1}^{N_i}$ for $x_j^{(i)} \sim \mu_i$. Applications where this problem arises are surveys broken into demographic or location groups [11], topic modeling from a bag of words model [31], and flow cytometry and other measurements of cell or gene populations per person [6, 10, 32].

*Department of Mathematics, University of California, San Diego, CA (cmoosmuller@ucsd.edu, acloninger@ucsd.edu).

[†]Halicioğlu Data Science Institute, University of California, San Diego, CA

The most natural way to solve the supervised learning problem on data $\{(\mu_i, y_i)\}_{i=1}^N$ is to embed μ_i into a (possibly infinite dimensional) Euclidean space and then apply traditional machine learning techniques on this embedding. Simple versions of this embedding would be through moments $\mu_i \mapsto \mathbb{E}_{X \sim \mu_i}[X]$ [22], or through a mean embedding $\mu_i \mapsto \mathbb{E}_{X \sim \mu_i} K(\cdot, X)$ for some kernel K [20]. However, these embeddings either throw away pertinent information about μ_i (e.g., higher order moments), or induce a complex nonlinear geometric relationship between distributions (e.g., $\|\mathbb{E}_{X \sim \mu(x)} K(\cdot, X) - \mathbb{E}_{X \sim \mu(x-\tau)} K(\cdot, X)\| \approx \|\mathbb{E}_{X \sim \mu(x)} K(\cdot, X) - \mathbb{E}_{X \sim \mu(x-2\tau)} K(\cdot, X)\|$ for τ significantly larger than the bandwidth of the kernel). These issues motivate the need for a transformation that is both injective and induces a simple geometric structure in the embedding space, so that one can learn an easy classifier.

The natural distance between distributions is Wasserstein-2 distance [29], where the distance between distributions μ and ν is

$$W_2(\mu, \nu)^2 = \min_{T \in \Pi_\mu^\nu} \int \|T(x) - x\|^2 d\mu(x), \quad (1)$$

where Π_μ^ν is the collection of all measure preserving maps from μ to ν . The argmin of (1) is referred to as the “optimal transport map” and we denote it by T_μ^ν (see Section 2 for a full description). Wasserstein distance is a more natural distance between distributions as it is a metric on distributions (unlike distances between a finite number of moments as above) and the distance does not saturate as the distributions move further apart (unlike mean embeddings as described above). Optimal transport has been of significant importance in machine learning, including as a cost for generative models [4], natural distances between images [26], pattern discovery for data cubes of neuronal data [19], and general semi-supervised learning [28]. There are two main drawbacks to optimal transport in machine learning. The first is that the computation of each transport map is slow, though this has motivated a number of approximations for computational speed up [12, 27, 16]. The second drawback is that it is difficult to incorporate supervised learning into optimal transport, as the distance is defined for a pre-defined cost function and eq. (1), as stated, does not generate a feature embedding of μ and ν that can be fed into traditional machine learning techniques.

This motivated the introduction of Linear Optimal Transportation (LOT) [30]. LOT is a set of transformations based on optimal transport maps, which map a distributions μ to the optimal transport map that takes a fixed reference distribution σ to μ :

$$\mu \mapsto T_\sigma^\mu. \quad (2)$$

The power of this transform lies in the fact that the nonlinear space of distributions is mapped into the linear space of L^2 functions. In addition, eq. (2) is an embedding with convex image.

In 1D, the optimal transport map is simply the generalized cdf of the distribution (if $\sigma = \text{Unif}([0, 1])$ this is exactly the traditional cdf). In [23], the

authors define the LOT as the Cumulative Distribution Transform (CDT), and the main theory and applications presented in [23] concern linear separability of data consisting of 1-dimensional densities.

However, LOT is more complicated on \mathbb{R}^n for $n > 1$. For $n = 1$, the cdf is the only measure preserving map from μ_i to σ , and it can be computed explicitly. This is not the case for $n > 1$: There are a large number of measure preserving maps, with the optimal transport map being the map that requires minimal work, see (1). Similarly, there are a much larger family of potential simple continuous perturbations that can be done to μ_i when $n > 1$ (e.g., sheerings, rotations) than exist for $n = 1$.

In [14], the CDT is combined with the Radon transform to apply results from [23] in general dimensions $n > 1$. While this construction can be considered a variant of LOT, a linear separability result for LOT in $n > 1$ is still missing. A proof of linear separability in LOT space for $n > 1$ is one of the main contributions of this paper (see Section 1.1).

The LOT embedding eq. (2) comes with yet another advantage. One can define a distance between two distributions μ_i and μ_j as the L^2 -norm of their images under LOT:

$$W_2^{\text{LOT}}(\mu_i, \mu_j)^2 := \|T_\sigma^{\mu_i} - T_\sigma^{\mu_j}\|_\sigma^2 = \int \|T_\sigma^{\mu_i}(x) - T_\sigma^{\mu_j}(x)\|^2 d\sigma(x).$$

In this paper, we prove that W_2 equals W_2^{LOT} if the family of distributions μ_i is generated by shifts and scalings of a fixed distribution μ . We further show that W_2 is well approximated by W_2^{LOT} for perturbations of shift and scalings (see Section 1.1).

We wish to highlight the computational importance of establishing approximate equivalence between LOT distance and Wasserstein-2 distance. Given N distributions, computing the exact Wasserstein-2 distance between all distributions naively requires computing $\binom{N}{2}$ expensive OT optimization problems. However, if the distributions come from a family of distributions generated by perturbations of shifts and scalings, one can instead compute N expensive OT optimization problems mapping each distribution to σ and compute $\binom{N}{2}$ cheap Euclidean distances between the transport maps, and this provably well approximates the ground truth distance matrix. In addition, the LOT embedding can be combined with algorithms such as Sinkhorn [12] to further improve the computational speed.

1.1 Main contributions

The main contributions of this paper are as follows:

- We establish the following with regards to LOT distance:

Theorem (Informal Statement of Theorem 4.4). *If μ and ν are ε -perturbations by shifts and scalings of one another, then*

$$W_2(\mu, \nu) \leq W_2^{\text{LOT}}(\mu, \nu) \leq W_2(\mu, \nu) + C_\sigma \varepsilon + \overline{C}_\sigma \varepsilon^{1/2}.$$

In particular, this implies that the LOT embedding is an isometry on the subset of measures related via shifts and scalings, i.e. when $\varepsilon = 0$.

- We establish the following with regards to building simple classifiers:

Theorem (Informal Statement of Theorem 5.4). *If $\mathcal{P} = \{\mu_i : y_i = 1\}$ are ε -perturbations of shifts and scalings of μ , and $\mathcal{Q} = \{\nu_i : y_i = -1\}$ are ε -perturbations of shifts and scalings of ν , and \mathcal{P} and \mathcal{Q} have a small minimal distance depending on ε (and satisfy a few technical assumptions), then \mathcal{P} and \mathcal{Q} are linearly separable in the LOT embedding space.*

- We demonstrate that in applications to MNIST images, the LOT embedding space is near perfectly linearly separable between classes of images and LOT distances match the theory.
- Of note to the optimal transport community, we establish in Corollary A.7 that the LOT related map

$$h \mapsto T_\sigma^{h_\# \mu},$$

where $h_\# \mu$ denotes the pushforward of μ under h , can achieve Hölder-type regularity. This result complements [13], where it is shown that 1/2-Hölder regularity can be achieved by the time-dependent map $t \mapsto T_\sigma^{\mu_t}$, for a curve of measures μ_t .

We wish to note that a week prior to upload of this paper, [1] was posted on arXiv. In [1], the authors prove that the LOT embeds a convex set of shifts and scalings (or for any compatible transformations, see our eq. (8) and Lemma 3.4) of a fixed distribution into a convex set in LOT space. This is a key part of the proof of our Theorems 5.3 and B.4, which we derived concurrently to [1]. We also derive these for any compatible transformations (see Appendix B). We have chosen to leave our proofs as is, and acknowledge the uploading of [1] here.

2 Preliminaries: Optimal Mass Transport

Let $\mathcal{P}(\mathbb{R}^n)$ be the set of probability measures on \mathbb{R}^n . By $\mathcal{P}_2(\mathbb{R}^n)$ we denote those measures in $\mathcal{P}(\mathbb{R}^n)$ with bounded second moment, i.e. $\sigma \in \mathcal{P}(\mathbb{R}^n)$ that satisfy

$$\int \|x\|_2^2 d\sigma(x) < \infty.$$

For $\sigma \in \mathcal{P}_2(\mathbb{R}^n)$ we also consider the space $L^2(\mathbb{R}^n, \sigma)$ with norm

$$\|f\|_\sigma^2 = \int \|f(x)\|_2^2 d\sigma(x).$$

In case of the L^2 -norm with respect to the Lebesgue measure λ , we simply write $\|f\|$.

For a map $T : \mathbb{R}^n \rightarrow \mathbb{R}^n$ and a measure σ we define the *pushforward measure* $T_{\#}\sigma$ by

$$T_{\#}\sigma(A) = \sigma(T^{-1}(A)),$$

where $A \subset \mathbb{R}^n$ is measurable and $T^{-1}(A)$ denotes the preimage of A under T .

If $\sigma \in \mathcal{P}_2(\mathbb{R}^n)$ is absolutely continuous with respect to the Lebesgue measure λ , which we denote by $\sigma \ll \lambda$, then there exists a density $f_{\sigma} : \mathbb{R}^n \rightarrow \mathbb{R}$ such that

$$\sigma(A) = \int_A f_{\sigma}(x) d\lambda(x), \quad A \subseteq \mathbb{R}^n \text{ measurable.} \quad (3)$$

In terms of densities, the pushforward relation $\nu(A) = \sigma(T^{-1}(A))$ is given by

$$\int_{T^{-1}(A)} f_{\sigma}(x) d\lambda(x) = \int_A f_{\nu}(y) d\lambda(y), \quad A \subseteq \mathbb{R}^n \text{ measurable.} \quad (4)$$

In case the map T is invertible and differentiable, we can rewrite (4) as

$$f_{\nu}(y) = f_{\sigma}(T^{-1}(y)) |\det D_y T^{-1}|. \quad (5)$$

Given two measures σ, ν , there can exist many maps T that push σ to ν . Therefore one seeks to impose yet another condition to make this map unique. In the theory of optimal transport [29], uniqueness is obtained via solving an optimization problem. The map T is required to minimize a cost function of the form

$$\int c(T(x), x) d\sigma(x), \quad (6)$$

under the constraint $T_{\#}\sigma = \nu$. In this paper we consider the cost $c(x, y) = \|x - y\|_2^2$. Other cost functions are possible as well, most notably, p -norms can be studied instead of 2-norms [29]. If the optimization has a solution, then

$$W_2(\sigma, \nu)^2 = \min_{T: T_{\#}\sigma = \nu} \int \|T(x) - x\|_2^2 d\sigma(x)$$

is the 2-*Wasserstein distance* between the measures σ and ν . In this paper we will refer to W_2 as *the* Wasserstein distance, as we only consider this case. The map T that minimizes (6) is called *optimal transport map*.

We introduce the notation T_{σ}^{ν} to denote the optimal transport map from σ to ν . With this notation we have the identity

$$W_2(\sigma, \nu) = \|T_{\sigma}^{\nu} - \text{Id}\|_{\sigma}.$$

We now cite a result concerning existence and uniqueness of the optimal transport map which is used throughout this paper.

Theorem 2.1 ([5], formulation taken from [25]). *Let $\sigma, \nu \in \mathcal{P}_2(\mathbb{R}^n)$ and consider the cost function $c(x, y) = \|x - y\|_2^2$. If σ is absolutely continuous with respect to the Lebesgue measure, then there exists a unique map $T \in L^2(\mathbb{R}^n, \sigma)$ pushing σ to ν , which minimizes (6). Furthermore, the map T is uniquely defined as the gradient of a convex function φ , $T(x) = \nabla\varphi(x)$, where φ is the unique (up to an additive constant) convex function such that $(\nabla\varphi)_{\#}\sigma = \nu$.*

There exist many generalizations of this result, for example to more general cost functions, or to Riemannian manifolds [5, 18, 29, 3].

3 Linear Optimal Transportation and its properties

In this section we introduce the *Linear Optimal Transportation (LOT)* as defined in [30] and present its basic properties.

LOT is an embedding of $\mathcal{P}_2(\mathbb{R}^n)$ into the linear space $L^2(\mathbb{R}^n, \sigma)$ based on a fixed measure σ . It is defined as

$$\nu \mapsto T_\sigma^\nu. \quad (7)$$

The power of this embedding lies in the fact that the target space is linear. This allows to apply linear methods to inherently nonlinear problems in $\mathcal{P}_2(\mathbb{R}^n)$ (see, for example, the application to classification problems in Section 5 and [23]).

The map eq. (7) has been studied by others authors as well, mainly with respect to regularity, see [13, 17]. In particular, the fact that 1/2-Hölder regularity of a time-dependent version of eq. (7) is achievable [13] is very useful for our purpose (see Appendix A).

We now define LOT and summarize its basic properties.

Definition 3.1 (Linear Optimal Transportation [30]). *Fix a measure $\sigma \in \mathcal{P}_2(\mathbb{R}^n)$, $\sigma \ll \lambda$. We define the Linear Optimal Transportation (LOT), F_σ , which assigns a function in $L^2(\mathbb{R}^n, \sigma)$ to a measure in $\mathcal{P}_2(\mathbb{R}^n)$:*

$$F_\sigma(\nu) = T_\sigma^\nu, \quad \nu \in \mathcal{P}_2(\mathbb{R}^n).$$

We now show that LOT is an embedding with convex image:

Lemma 3.2. *For fixed $\sigma \in \mathcal{P}_2(\mathbb{R}^n)$, $\sigma \ll \lambda$, we have the following*

1. F_σ embeds $\mathcal{P}_2(\mathbb{R}^n)$ into $L^2(\mathbb{R}^n, \sigma)$;
2. the image $F_\sigma(\mathcal{P}_2(\mathbb{R}^n))$ is convex in $L^2(\mathbb{R}^n, \sigma)$.

Proof. The proof is an application of Theorem 2.1. We show details in Section C. \square

We introduce a compatibility condition between LOT and the pushforward operator, which is one of the key ingredients for the results in Section 4 and Section 5.

Fix two measures $\sigma, \mu \in \mathcal{P}_2(\mathbb{R}^n)$, $\sigma \ll \lambda$. F_σ is called *compatible* with μ -pushforwards of a set of functions $\mathcal{H} \subseteq L^2(\mathbb{R}^n, \mu)$ if for every $h \in \mathcal{H}$ we have

$$F_\sigma(h_\# \mu) = h \circ F_\sigma(\mu). \quad (8)$$

Remark 3.3. For $\sigma = \mu$, the compatibility condition reads as $T_\sigma^{h_\#} \sigma = h$. This means that a function h is required to be the optimal transport from σ to $h_\# \sigma$. This is a rather strong condition, and not satisfied for a general function h . Nevertheless, we show below that it is satisfied for shifts and scalings.

The compatibility condition can also be understood in terms of operators. The pushforward operator $h \mapsto h_\# \sigma$, is left-inverse to F_σ . The compatibility condition requires that it is also right-inverse.

For $a \in \mathbb{R}^n$ denote by $S_a(x) = a + x$ the shift by a . Similarly, for $c > 0$ denote by $R_c(x) = cx$ the scaling by c . We denote by $\mathcal{E} := \{S_a : a \in \mathbb{R}^n\} \cup \{R_c : c > 0\}$ the set of all shifts and scalings.

Lemma 3.4 (Compatibility on \mathbb{R} and with shifts and scalings). *Let $\sigma, \mu \in \mathcal{P}_2(\mathbb{R}^n)$, $\sigma \ll \lambda$.*

1. *If $n = 1$, i.e. on \mathbb{R} , F_σ is compatible with μ -pushforwards of monotonically increasing functions.*
2. *For general $n \geq 1$, F_σ is compatible with μ -pushforwards of shifts and scalings, i.e. functions in \mathcal{E} .*

Proof. The proof is an application of Theorem 2.1, we show details in Section C. □

4 Approximation of the Wasserstein distance by LOT embedding

From Lemma 3.2 we know that LOT embeds $\mathcal{P}_2(\mathbb{R}^n)$ into $L^2(\mathbb{R}^n, \sigma)$. In general, this embedding is not an isometry.

In this section we derive the error that occurs when approximating the Wasserstein distance by the L^2 distance obtained in the LOT embedding. We are thus interested in the accuracy of the following approximation:

$$W_2(\mu, \nu) \approx \|F_\sigma(\mu) - F_\sigma(\nu)\|_\sigma. \quad (9)$$

Note that if $W_2(\mu, \nu)$ is approximated well by $\|F_\sigma(\mu) - F_\sigma(\nu)\|_\sigma$, LOT is very powerful, as the Wasserstein distance between k different measures can be computed from only k transports instead of $\binom{k}{2}$. Indeed, in this section we show that eq. (9) is exact, i.e. the LOT embedding is an isometry, for two important cases: On \mathbb{R} , and on \mathbb{R}^n if both μ and ν are pushforwards of a fixed measure under shifts and scalings. We further show that it is almost exact for pushforwards of functions close to shifts and scalings.

We first establish an approximation result:

Theorem 4.1. *Let $\sigma, \mu, \nu \in \mathcal{P}_2(\mathbb{R}^n)$, $\sigma, \mu \ll \lambda$, then we have*

$$W_2(\mu, \nu) \leq \|F_\sigma(\mu) - F_\sigma(\nu)\|_\sigma \leq W_2(\mu, \nu) + \|T_\mu^\nu - T_\sigma^\nu \circ T_\mu^\sigma\|_\mu.$$

We also have an upper bound by the triangle inequality

$$\|F_\sigma(\mu) - F_\sigma(\nu)\|_\sigma \leq W_2(\mu, \sigma) + W_2(\sigma, \nu).$$

Proof. By the change-of-variables formula we have

$$\|F_\sigma(\mu) - F_\sigma(\nu)\|_\sigma = \|T_\sigma^\mu - T_\sigma^\nu\|_\sigma = \|\text{Id} - T_\sigma^\nu \circ T_\mu^\sigma\|_\mu \quad (10)$$

Since $T_\sigma^\nu \circ T_\mu^\sigma$ pushes μ to ν , $W_2(\mu, \nu) \leq \|F_\sigma(\mu) - F_\sigma(\nu)\|_\sigma$ follows.

For the first upper bound on $\|F_\sigma(\mu) - F_\sigma(\nu)\|_\sigma$ note the following

$$\|\text{Id} - T_\sigma^\nu \circ T_\mu^\sigma\|_\mu \leq \|\text{Id} - T_\mu^\nu\|_\mu + \|T_\mu^\nu - T_\sigma^\nu \circ T_\mu^\sigma\|_\mu \leq W_2(\mu, \nu) + \|T_\mu^\nu - T_\sigma^\nu \circ T_\mu^\sigma\|_\mu.$$

The second upper bound by $W_2(\mu, \sigma) + W_2(\sigma, \nu)$ follows from the triangle inequality. \square

Theorem 4.1 shows that the error occurring in the LOT approximation of the Wasserstein distance is determined by the L^2 -error between the map $T_\sigma^\mu \circ T_\mu^\sigma$ and the correct transport map T_μ^ν . This means that the LOT embedding replaces the transport T_μ^ν by $T_\sigma^\mu \circ T_\mu^\sigma$ and computes the Wasserstein distance from this map. The correct Wasserstein distance

$$W_2(\mu, \nu) = \|T_\mu^\nu - \text{Id}\|_\mu$$

is replaced by the LOT approximation as

$$W_2(\mu, \nu) \approx \|T_\sigma^\nu \circ T_\mu^\sigma - \text{Id}\|_\mu = \|T_\sigma^\mu - T_\sigma^\nu\|_\sigma.$$

Theorem 4.1 shows that in case the relation

$$T_\mu^\nu = T_\sigma^\nu \circ T_\mu^\sigma \quad (11)$$

is satisfied, the LOT embedding is an isometry. Also, if eq. (11) is satisfied up to an error $\varepsilon > 0$, then ε is also the maximal error between the LOT embedding and the correct Wasserstein distance.

We prove in Section D that compatibility of F_σ with μ -pushforwards eq. (8) implies the relation eq. (11) is satisfied. Therefore, $n = 1$ and pushforwards of shifts and scalings on \mathbb{R}^n are our main examples for which F_σ is an isometry (see Theorems 4.2 and 4.3 below).

Yet eq. (11) is not satisfied in general. Using $T_\sigma^\nu \circ T_\mu^\sigma$ instead of T_μ^ν can be viewed as a kind of triangle inequality for transports. Instead of mapping directly from μ to ν , one has to go via σ . Nevertheless the LOT embedding approximates the Wasserstein distance better than the regular triangle inequality $W_2(\mu, \nu) \leq W_2(\mu, \sigma) + W_2(\sigma, \nu)$. This fact is well visible in the example discussed in Section 4.1.1. In particular, LOT has the following advantages over the triangle inequality:

1. Theorem 4.1 implies that the LOT embedding is upper bounded by the triangle inequality, i.e.

$$\|F_\sigma(\mu) - F_\sigma(\nu)\|_\sigma \leq W_2(\mu, \sigma) + W_2(\sigma, \nu).$$

2. The LOT embedding is an isometry on \mathbb{R} , i.e. if $n = 1$, see Theorem 4.2.
3. For $n \geq 1$, the LOT embedding is an isometry if both μ and ν are pushforwards of a fixed measure by shifts or scalings (Theorem 4.3).
4. The LOT embedding is close to an isometry for pushforwards of a fixed measure by functions close to scalings and shifts (Theorem 4.4).

4.1 LOT as an isometry

Below, we establish on both \mathbb{R} and \mathbb{R}^n that LOT distances between compatible transformations of a distribution are isometric to Wasserstein-2 distances. The importance of these results are demonstrated in Section 4.1.1.

Theorem 4.2. *On \mathbb{R} , F_σ is an isometry.*

Proof. We proof in Lemma D.1 that compatibility of F_σ with μ -pushforwards implies eq. (11). Thus the theorem follows from Lemma 3.4. \square

Recall that we denote by $\mathcal{E} = \{S_a : a \in \mathbb{R}^n\} \cup \{R_c : c > 0\}$ the set of all shifts and scalings.

Theorem 4.3. *Consider a set of functions consisting of shifts and scalings, $\mathcal{H} \subseteq \mathcal{E}$, and consider a set pushforward measures of a fixed measure $\mu \in \mathcal{P}_2(\mathbb{R}^n)$, $\mu \ll \lambda$, by functions in \mathcal{H} :*

$$\mathcal{H} \star \mu := \{h_\# \mu : h \in \mathcal{H}\}.$$

For another measure $\sigma \in \mathcal{P}_2(\mathbb{R}^n)$, $\sigma \ll \lambda$, and $\nu_1 = h_{1\#} \mu, \nu_2 = h_{2\#} \mu \in \mathcal{H} \star \mu$, we have

$$W_2(\nu_1, \nu_2) = \|F_\sigma(\nu_1) - F_\sigma(\nu_2)\|_\sigma = \|h_1 - h_2\|_\mu.$$

This means that F_σ restricted to $\mathcal{H} \star \mu$ is an isometry.

Proof. We proof in Lemma D.1 that compatibility of F_σ with μ -pushforwards implies eq. (11). Thus the theorem follows from Lemma 3.4. \square

Note that if $\sigma = \mu$ and $h \in \mathcal{E}$, and $g \in L^2(\mathbb{R}^n, \mu)$, then for $\nu_1 = h_\# \mu$ and $\nu_2 = g_\# \mu$ we also get

$$W_2(\nu_1, \nu_2) = \|F_\mu(\nu_1) - F_\mu(\nu_2)\|_\mu = \|h - g\|_\mu.$$

4.1.1 Example: Shifted and scaled uniform distributions

To illustrate how the LOT embedding can be used to approximate the Wasserstein distance, we consider shifted and scaled uniform distributions on a regular grid, see Figure 1. In this set up the LOT embedding is an isometry (Theorem 4.3).

Consider uniform distributions $\nu_j, j = 1, \dots, 5$ (blue distributions in Figure 1) which are arranged on a grid in $[-3, 3]^2$. The grid is indicated by the

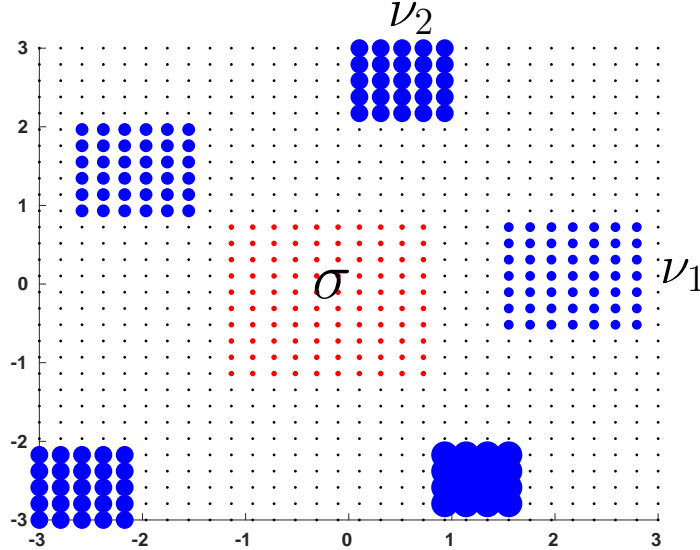


Figure 1: In blue: Shifted and scaled uniform distributions $\nu_j, j = 1, \dots, 5$ on a regular grid in $[-3, 3]^2$. In red: Reference density σ (uniform distribution) used to approximate the Wasserstein distance between the blue uniform densities via the LOT embedding.

black dots in Figure 1. Note that each $\nu_j, j = 1, \dots, 5$, can be viewed as a shifted and scaled version of a fixed uniform distribution μ .

To obtain the ground truth pairwise distances between the blue uniform distributions $\nu_j, j = 1, \dots, 5$ of Figure 1, we use a linear program to compute the exact optimal transport (using G. Peyré’s *Numerical Tours* [24]). The pairwise W_2 distance matrix is shown in the left plot of Figure 2, labeled as “ W_2 ground truth”. Note that in order to obtain this pairwise distance matrix, $\binom{5}{2}$ optimal transport computations are necessary.

We now use the LOT embedding to compute the W_2 distance between the blue uniform distributions of Figure 1. We first pick a reference density σ , which is the red uniform distribution in Figure 1. We compute all exact optimal transports from σ to all $\nu_j, j = 1, \dots, 5$, again using a linear program. Note that we only need to compute 5 optimal transports (instead of $\binom{5}{2}$). Since all blue uniform distributions can be considered shifts and scalings of a fixed uniform distribution μ , we can use the fact that the LOT embedding is an isometry (Theorem 4.3). Thus $W_2(\nu_i, \nu_j)$ can be computed by $\|T_\sigma^{\nu_i} - T_\sigma^{\nu_j}\|_2$ where $i, j \in \{1, \dots, 5\}$. The distance matrix resulting from this computation is shown in the middle plot of Figure 2, labeled as “ W_2 from LOT embedding”.

We also compute the distance matrix obtained by using the triangle inequality $W_2(\nu_i, \sigma) + W_2(\sigma, \nu_j)$ to approximate $W_2(\nu_i, \nu_j)$, for $i, j \in \{1, \dots, 5\}$. In this case, only 5 optimal transports need to be computed, but the result is

inaccurate, see the right plot of Figure 2.

Since the LOT embedding is an isometry for shifted and scaled versions of a fixed distribution μ , the distance matrices obtained from the LOT embedding equals the ground truth (compare left and middle plot of Figure 2). Indeed, for this example, the maximum relative error is

$$\text{relativeError}(\text{LOT}, \text{LP}) = \max_{i,j=1,\dots,5} \frac{|W_2^{\text{LOT}}(\nu_i, \nu_j) - W_2^{\text{LP}}(\nu_i, \nu_j)|}{W_2^{\text{LP}}(\nu_i, \nu_j)} = 0.0049, \quad (12)$$

where W_2^{LOT} denotes the Wasserstein distance computed via the LOT embedding, and W_2^{LP} denotes the Wasserstein distance computed by a linear program (LP). Therefore, in this example, the LOT embedding approximates the Wasserstein distance with very good accuracy, while needing only k instead of $\binom{k}{2}$ optimal transport computations (where k is the number of distributions).

Figure 2 clearly shows that the triangle inequality is not suitable for approximating the Wasserstein distance in this example. Indeed, the relative error between the ground truth distance matrix and the distance matrix obtained by using the triangle inequality is $\text{relativeError}(\text{triangle}, \text{LP}) = 0.9$.

4.2 LOT is close to an isometry under perturbations of shifts and scalings

It is important to note that in most applications, distributions are not exact shifts or scalings of one another. There always exist perturbations of distributions, whether it is rotation, stretching, or sheering. Thus, it is important to consider the behavior of LOT under such perturbations, and demonstrate that the LOT distance continues to be a quasi-isometry with respect to Wasserstein-2 distance and that the deformation constants depend smoothly on the size of the perturbation.

Let $\mu \in \mathcal{P}_2(\mathbb{R}^n)$, $R > 0$, and $\varepsilon > 0$. Recall that we denote by \mathcal{E} the set of all shifts and scalings. We define the sets

$$\mathcal{E}_{\mu,R} = \{h \in \mathcal{E} : \|h\|_{\mu} \leq R\} \quad (13)$$

and

$$\mathcal{G}_{\mu,R,\varepsilon} = \{g \in L^2(\mathbb{R}^n, \mu) : \exists h \in \mathcal{E}_{\mu,R} : \|g - h\|_{\mu} \leq \varepsilon\}. \quad (14)$$

This can be thought of as the ε tube around set of shifts and scalings, or as the set of almost compatible transformations.

Theorem 4.4. *Let $\sigma, \mu \in \mathcal{P}_2(\mathbb{R}^n)$, $\sigma, \mu \ll \lambda$. Assume that σ, μ satisfy the assumptions of Caffarelli's regularity theorem (Theorem A.1).*

Let $R > 0, \varepsilon > 0$. Then for $g_1, g_2 \in \mathcal{G}_{\mu,R,\varepsilon}$ we have

$$0 \leq \|F_{\sigma}(g_{1\#}\mu) - F_{\sigma}(g_{2\#}\mu)\|_{\sigma} - W_2(g_{1\#}\mu, g_{2\#}\mu) \leq C_{\sigma,\mu,R}\varepsilon + \overline{C}_{\sigma,\mu,R}\varepsilon^{1/2},$$

where $C_{\sigma,\mu,R}, \overline{C}_{\sigma,\mu,R}$ are constants depending on σ, μ and R .

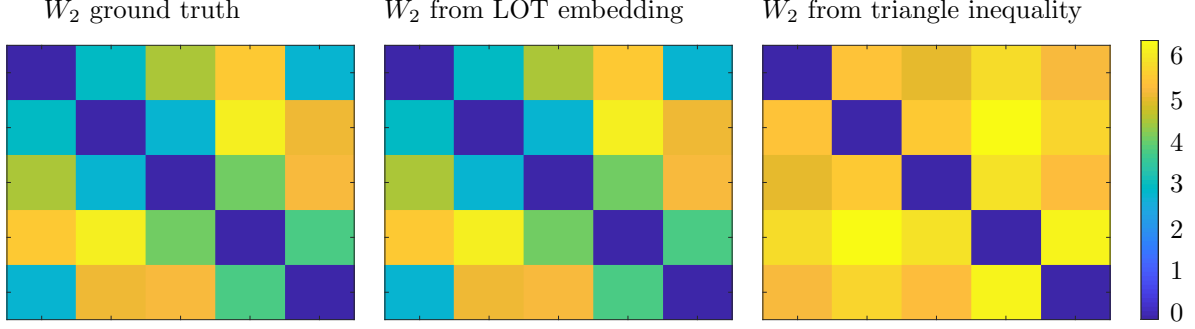


Figure 2: *Left:* Ground truth Wasserstein distance matrix between the blue uniform distributions in Figure 1. The Wasserstein distance between all blue uniform distributions is computed using a linear program. This requires the computation of $\binom{5}{2}$ optimal transports. *Middle:* Wasserstein distance matrix between the blue uniform distributions in Figure 1 computed by the LOT embedding. The Wasserstein distance between all blue uniform distributions $\nu_j, j = 1, \dots, 5$ and the reference density σ (red uniform distribution) is computed by a linear program. The distance between two blue uniform distributions $W_2(\nu_i, \nu_j)$ is then approximated by the 2-norm as $\|T_\sigma^{\nu_j} - T_\sigma^{\nu_i}\|_2, i, j = 1, \dots, 5$. This procedure only needs to compute 5 optimal transports and is very accurate. *Right:* The distance matrix obtained by approximating the Wasserstein distance between two blue uniform distributions, $W_2(\nu_i, \nu_j)$, via the triangle inequality $W_2(\nu_i, \sigma) + W_2(\sigma, \nu_j), i, j = 1, \dots, 5$. Here only 5 optimal transports need to be computed, but the result is very inaccurate.

Proof. The proof can be found in Section D. \square

We mention that through the application of Corollary A.7, the constants appearing in this theorem can be characterized explicitly, see Section D.

The theorem states that for functions close to “ideal” functions (shifts and scalings), the LOT embedding is an almost isometry. In the next section we establish this result numerically.

4.2.1 Example: Perturbations of MNIST data

We apply the LOT embedding to approximate the Wasserstein distance between shifts and perturbations of a fixed digit from the MNIST data set [15]. The aim of this example is to study the error bound of Theorem 4.4 numerically.

We pick a 1 from the MNIST data set (top left plot of Figure 3). We then apply a shift to this image, see the top middle plot of Figure 3. From Section 4.1 we know that the LOT embedding is an isometry under shifts. In order to study the perturbation result (Theorem 4.4), after the shift, we rotate the 1 by angles of $0^\circ - 45^\circ$, as shown in Figure 3. Note that the rotations are implemented via

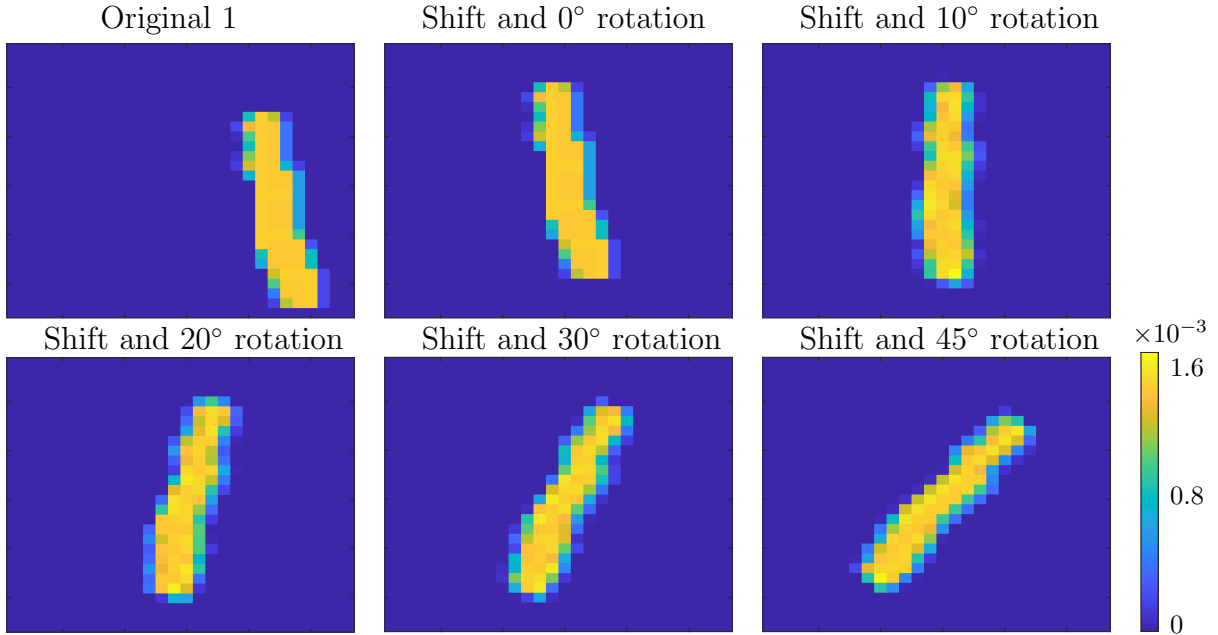


Figure 3: We pick a 1 from the MNIST data set [15] (top left). We then apply a shift and perturbations via rotation around an angle ($0^\circ - 45^\circ$). Rotations are implemented via MATLAB’s “imrotate” function which uses interpolation. We then compute the Wasserstein-2 distance between the original 1 (top left) and all the other 1s both via the LOT embedding (using as reference density σ an isotropic Gaussian) and via the exact linear program. The error estimate is shown in Figure 4.

MATLAB’s “imrotate” function which introduces an additional error through the interpolation used in this function. On the other hand, shifts can be carried out without numerical errors via MATLAB’s “circshift” function.

Denoting the original 1 by μ , all the other 1s can be considered as $(L_\theta \circ S_a)_\# \mu$, where S_a is the shift by a fixed vector a and L_θ is the rotation matrix

$$L_\theta = \begin{bmatrix} \cos(\theta) & -\sin(\theta) \\ \sin(\theta) & \cos(\theta) \end{bmatrix}$$

with $\theta \in [0, \pi/4]$. Note that the functions $L_\theta \circ S_a$ are perturbations as discussed in Section 4.2.

We now compute the Wasserstein-2 distance between the original 1 and all the shifted and rotated 1s. We first use the LOT embedding with reference density σ an isotropic Gaussian as shown in Figure 6 (left plot). Then we compute the exact Wasserstein-2 distances with a linear program [24].

To study Theorem 4.4, we compare the absolute error between the LOT approximation and the exact W_2 distances to the size of perturbation applied to the shift, i.e. we are interested in

$$|W_2^{\text{LOT}}(\mu, (L_\theta \circ S_a)_\# \mu) - W_2^{\text{LP}}(\mu, (L_\theta \circ S_a)_\# \mu)| \quad (15)$$

versus $\sqrt{\varepsilon}$ and ε with

$$\varepsilon = \|L_\theta - \text{Id}\|_\mu. \quad (16)$$

(Note that the shift cancels). Instead of ε , we actually compute $\|L_\theta - \text{Id}\|_\sigma$, since this can be conveniently computed with the Frobenius norm (see Remark 4.5). Note that this alteration just adds another constant to the estimate in Theorem 4.4 in terms of ε and $\sqrt{\varepsilon}$.

We plot the absolute error eq. (15), ε and $\sqrt{\varepsilon}$ as functions of the angle θ in Figure 4. It is clear from this figure that the error induced by angle rotation is below the error established in Theorem 4.4. In particular, note that the constants derived in Theorem 4.4 are not necessarily smaller than 1.

It is also visible that the error increases with the angle, which shows that the farther away from a compatible function (i.e. shift in this case) the larger the error gets. Also note that with 0° rotation, the error is 0 which relates to the fact that for simple shifts (without rotation), LOT is an isometry (Theorem 4.4).

Remark 4.5. *The norm in eq. (16) can be computed as the Frobenius norm of the matrix $L_\theta - \text{Id}$. Indeed, for a symmetric matrix S we have that*

$$\mathbb{E}[x^T S x] = \text{trace}(S \Sigma) + m^T S m,$$

where $\mathbb{E}[x] = m$ and $\text{Var}(x) = \Sigma$.

Now for a linear operator L this implies

$$\|L\|_\sigma^2 = \mathbb{E}[x^T L^T L x] = \text{trace}(L^T L),$$

since $\mathbb{E}[x] = 0$ and $\text{Var}(x) = \text{Id}$ for σ an isotropic Gaussian.

4.3 Example: Error between different digits in MNIST data

We apply the LOT embedding to approximate the Wasserstein distance between different digits from the MNIST data set [15].

We pick one digit 1 and one 2 from [15] and shift them, see Figure 5. We thus create two classes of examples, shifted 1s (first row of Figure 5), and shifted 2s (second row of Figure 5).

For any choice of reference density σ , Theorem 4.3 implies that the Wasserstein distance equals the distance from the LOT embedding in each individual class, i.e. between all 1s, and between all 2s.

To compute the Wasserstein distance in the inbetween classes, i.e. between 1s and 2s, we are in a more complicated situation compared to Section 4.2.1, as 1s and 2s cannot be considered shift, scalings or perturbations of each other.

As in Section 4.1.1 and Section 4.2.1 we compute the ground truth Wasserstein distance between all 1s and 2s using a linear program ($\binom{6}{2}$ transports are computed). We then compute the Wasserstein distance from the reference density σ , which we choose as an isotropic Gaussian (see left plot in Figure 6), to

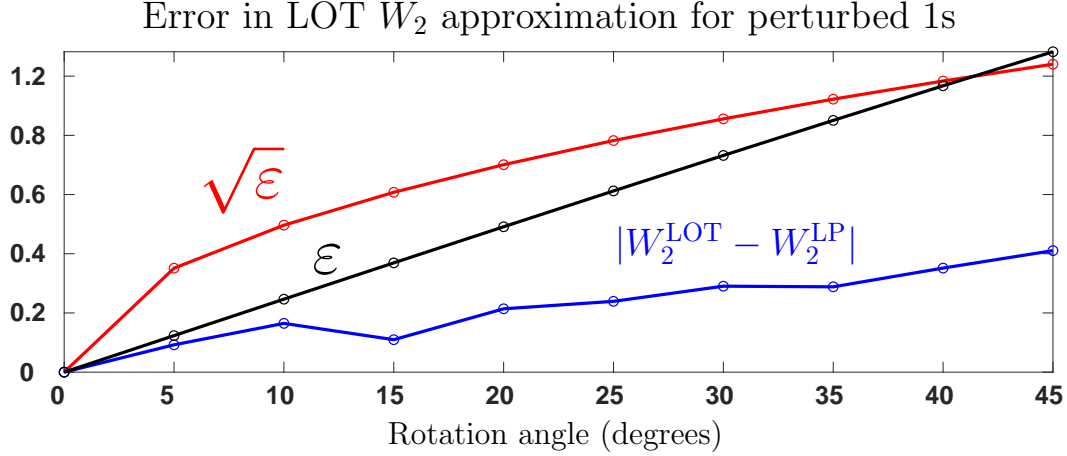


Figure 4: We compute the Wasserstein-2 distance between the 1 (top left in Figure 3) to all of the shifted and perturbed 1s in Figure 3. The perturbations are implemented as rotation of the shifted 1 by angles $\theta \in [0, \pi/4]$. We first approximate W_2 with the LOT embedding (using an isotropic Gaussian as reference density σ), labeled as W_2^{LOT} , and then compute the exact W_2 distance, W_2^{LP} , with a linear program. The absolute error $|W_2^{\text{LOT}} - W_2^{\text{LP}}|$ is compared to the error bound established in Theorem 4.4 as a function of the perturbation angle θ . This error bound depends on $\sqrt{\epsilon}$ and ϵ where ϵ is the deviation of the rotation from the identity, i.e. $\epsilon = \|L_\theta - \text{Id}\|_\sigma$. The deviation ϵ can be conveniently computed as the Frobenius norm of the matrix $L_\theta - \text{Id}$, see Remark 4.5.

all 1s and 2s. The Wasserstein distance between all characters is then approximated via the LOT embedding. This computation again involves only 6 optimal transports.

The relative error between the ground truth distance and the LOT embedding approximation is shown in the right plot of Figure 6. As expected, the error within each class (1s and 2s) is 0. The maximal inbetween classes relative error is 0.045, which is comparable to the example of rotations by $\theta = \pi/4$ as in Section 4.2.1.

5 Linear separability

In this section, we characterize the geometry of the LOT embedding space under families of compatible transformations in \mathcal{E} (i.e., shifts and scalings), as well as for approximately compatible transformations in $\mathcal{G}_{\lambda, R, \epsilon}$ (eq. (14)), where λ denotes the Lebesgue measure.

Recall from Theorem 4.3 that for a measure μ and a set of functions \mathcal{H} we denote by $\mathcal{H} \star \mu$ the set of all pushforwards of μ under \mathcal{H} , i.e.

$$\mathcal{H} \star \mu = \{h_\# \mu : h \in \mathcal{H}\}.$$

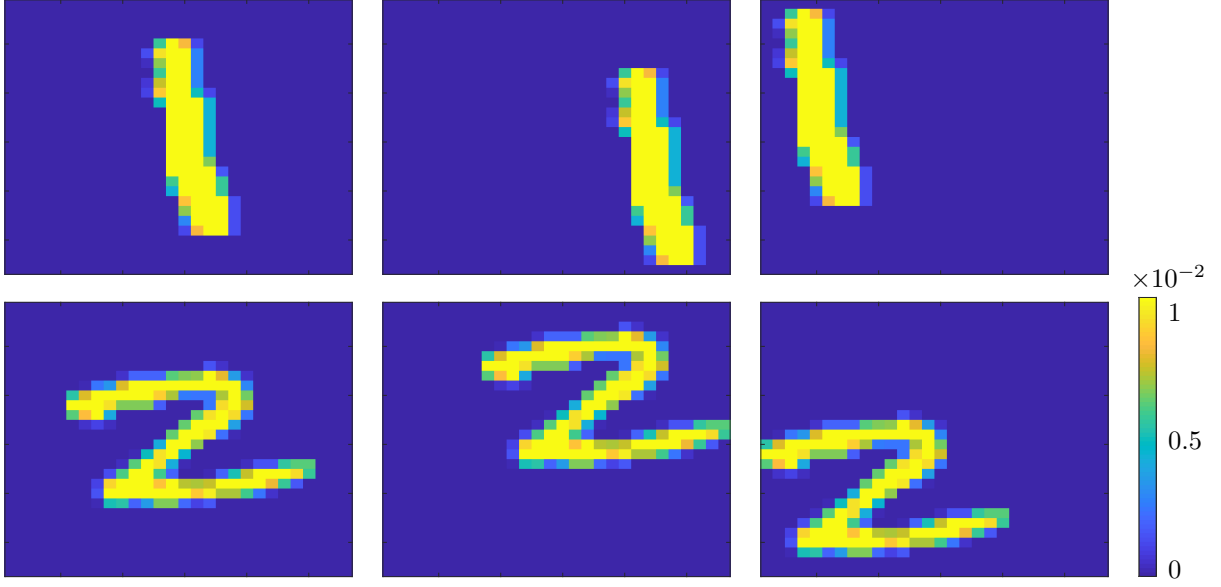


Figure 5: Handwritten characters from [15]. We pick one 1 and one 2 (first column), and shift them (second and third column). Shifts are implemented via MATLAB’s “circshift” function. We approximate the Wasserstein distance on this data set of shifted 1s and 2s using the LOT embedding. The relative error of the W_2 -approximation by the LOT embedding is shown in Figure 6.

In this section, we are mainly interested in conditions under which two families of distributions defined by pushforwards of $\mathcal{G} \subset \mathcal{G}_{\lambda, R, \varepsilon}$, $\mathcal{G} \star \mu$ and $\mathcal{G} \star \nu$, are linearly separable in the LOT embedding space.

Before stating the main results of this section, we briefly describe linear separability and its importance in machine learning. Linear separability of two disjoint sets in a Hilbert space implies the existence of a hyperplane $w(x) = b$ such that

$$\begin{aligned} \langle w, \mu_i \rangle &< b, & \forall \mu_i \in \mathcal{H} \star \mu \\ \langle w, \nu_i \rangle &> b, & \forall \nu_i \in \mathcal{H} \star \nu. \end{aligned}$$

The existence of such a hyperplane can be established through the Hahn-Banach separation theorem. The theorem simply assumes that the two sets $(\mathcal{H} \star \mu, \mathcal{H} \star \nu)$ are convex, and that one is closed and the other is compact [21].

Linear separability is a strong and important condition for many machine learning applications and supervised learning generally. This is because learning a linear classifier is very straightforward, and does not require many training points to accurately estimate $w(x)$. This implies that once the distributions are mapped to the LOT embedding space, it is possible to learn a classifier that perfectly separates the two families with only a small amount of labeled examples.

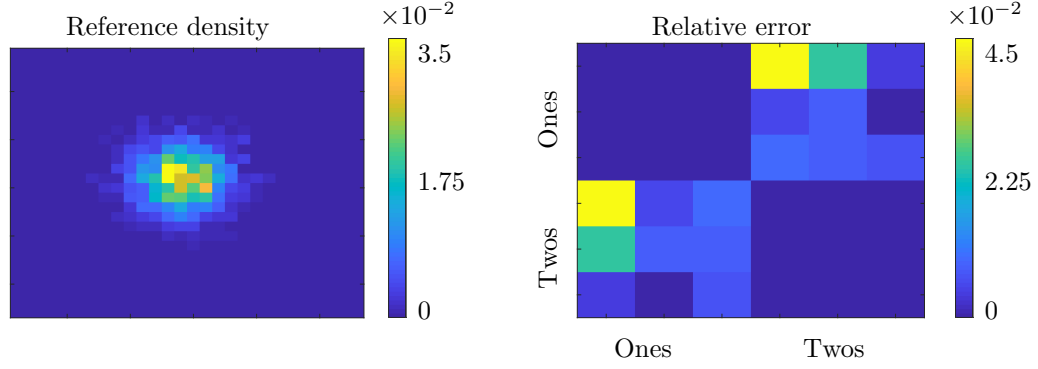


Figure 6: *Left:* The reference density σ (Gaussian) used in the LOT embedding to approximate the Wasserstein distances between all 1s and 2s of Figure 5. *Right:* Relative error between the ground truth Wasserstein distances of the data set from Figure 5 and the distances computed by the LOT embedding. The error is 0 in each individual class of 1s and 2s since the LOT embedding is an isometry on these subsets (Theorem 4.3). In the inbetween classes, i.e. between 1s and 2s, the error is comparable with the error in the example of rotated 1s with angle $\theta = \pi/4$, see Section 4.2.1.

We note that the result on $\mathcal{G}_{\lambda,\varepsilon,R}$ (Theorem 5.4) is the main result of this section, but we list several other results for completeness. We also note that, for ease of understanding, we frame all theorems in this section for subsets of shifts/scalings or perturbations of such. However, Theorems 5.3 and 5.4 actually have versions in Appendix B (Theorems B.4 and B.7, respectively) for the family of all compatible and approximately compatible transformations. Furthermore, in the case of $\mathcal{G}_{\lambda,\varepsilon,R}$ (Theorem 5.4), through Corollary A.7, we can give an explicit characterization of the minimal distance δ required between the two families of distributions, $\mathcal{G} \star \mu$ and $\mathcal{G} \star \nu$, to guarantee linear separability.

First, we note the separability result on \mathbb{R} , which is also proved in [23].

Theorem 5.1. *Let $\sigma, \mu, \nu \in \mathcal{P}_2(\mathbb{R})$, $\sigma \ll \lambda$, and let \mathcal{H} be a convex set of monotonically increasing functions $\mathbb{R} \rightarrow \mathbb{R}$. If $\mathcal{H} \star \mu$ is closed and $\mathcal{H} \star \nu$ is compact, and these two sets are disjoint, then $F_\sigma(\mathcal{H} \star \mu)$ and $F_\sigma(\mathcal{H} \star \nu)$ are linearly separable.*

Proof. The proof can be found in Section E. □

Remark 5.2. *Note that Theorem 5.1 is also proved in [23]. In [23], \mathbb{H} (equivalent to our \mathcal{H}) is defined as a convex subgroup of the monotonic functions (Definition 5.5 and Definition 5.6 (i)–(iii) of [23]). We are able to relax the assumption from subgroup to subset, however. Definition 5.5 of [23] also assumes differentiability of functions in \mathbb{H} , which is needed because constructions*

are considered from the viewpoint of densities, which means that (5) should hold. Since our approach uses the more general framework of measures rather than densities, we can drop this assumption.

Second, we establish simple conditions under which LOT creates linearly separable sets for distributions in $\mathcal{P}_2(\mathbb{R}^n)$. This effectively creates a parallel of Theorem 5.1 and Theorem 5.6 of [23] for the higher dimensional cases of LOT, and under the particular compatibility conditions required for higher dimensions. Theorem 5.3 states this for \mathcal{E} (shifts and scalings), and Theorem B.4 in the Appendix provides an equivalent form for subsets of arbitrary compatible transforms.

Theorem 5.3. *Let $\sigma, \mu, \nu \in \mathcal{P}_2(\mathbb{R}^n)$, $\sigma \ll \lambda$, and let $\mathcal{H} \subseteq \mathcal{E}$ and let \mathcal{H} be convex. If $\mathcal{H} \star \mu$ is closed and $\mathcal{H} \star \nu$ is compact, and these two sets are disjoint, then $F_\sigma(\mathcal{H} \star \mu)$ and $F_\sigma(\mathcal{H} \star \nu)$ are linearly separable.*

Proof. The proof can be found in Section E. \square

Finally, we establish the main result of this section, which covers approximately compatible transforms in $\mathcal{G}_{\lambda, \varepsilon, R}$, the ε tube around the bounded shifts and scalings $\mathcal{E}_{\lambda, R}$. Theorem 5.4 establishes the case for the tube around $\mathcal{E}_{\lambda, R}$, and Theorem B.7 establishes the condition for almost compatible transformations. In both cases to show linear separability in the LOT embedding space, one must now assume that the two families of distributions are not just disjoint, but actually have a nontrivial minimal distance. The benefit of restricting ourselves to $\mathcal{G}_{\lambda, \varepsilon, R}$, is that we can define a closed form expression for a sufficient minimal distance. This is done through the constant

$$\begin{aligned} \delta(\varepsilon, R, \sigma, \mu) := & \left(\sqrt{\frac{4R}{K_\mu^\sigma}} + 2 \right) \|f_\mu\|_\infty^{1/2} \varepsilon \\ & + \left(4R \|f_\mu\|_\infty^{1/2} \frac{W_2(\sigma, \mu) + R + \|\text{Id}\|_\mu}{K_\mu^\sigma} \right)^{1/2} \varepsilon^{1/2}, \end{aligned}$$

which is established from Corollary A.7. Note that K_μ^σ is defined in Definition A.2. A version of $\delta(\varepsilon, R, \sigma, \mu)$ also appears in characterizing the amount that LOT distance deviates from Wasserstein-2 distance (Theorem 4.4). A parallel of $\delta(\varepsilon, R, \sigma, \mu)$ could be established for any approximately compatible transformations by proving a result similar to Lemma A.5 for some compatible transformation other than shifts and scalings.

Theorem 5.4. *Let $\sigma, \mu, \nu \in \mathcal{P}_2(\mathbb{R}^n)$, $\sigma, \mu, \nu \ll \lambda$ and assume that σ, μ, ν satisfy the assumptions of Caffarelli's regularity theorem (Theorem A.1).*

Let $R > 0, \varepsilon > 0$. Consider $\mathcal{G} \subset \mathcal{G}_{\lambda, R, \varepsilon}$ and let \mathcal{G} be convex. Let $\delta = \max\{\delta(\varepsilon, R, \sigma, \mu), \delta(\varepsilon, R, \sigma, \nu)\}$.

If $\mathcal{G} \star \mu$ and $\mathcal{G} \star \nu$ are compact and $W_2(g_1 \star \mu, g_2 \star \nu) > 6\delta$ for all $g_1, g_2 \in \mathcal{G}$, then $F_\sigma(\mathcal{G} \star \mu)$ and $F_\sigma(\mathcal{G} \star \nu)$ are linearly separable.

Proof. The proof can be found in Section E. \square

Remark 5.5. *We note that each Theorem in this section can be trivially extended to an arbitrary set \mathcal{H} (or \mathcal{G}) that is not required to be convex, so long as their convex hulls $\text{conv}(\mathcal{H})$ (or $\text{conv}(\mathcal{G})$) satisfy the needed assumptions of closedness, compactness, and disjointness.*

5.1 Example: Linear separability of MNIST data set

We linearly separate two classes of digits from the MNIST data set [15] with LOT to verify the linear separability result (Theorem 5.4) numerically.

We consider the classes of 1s and 2s from the MNIST data set. Within each class, the digits can be considered as shifts, scalings and perturbations of each other. Therefore, via Theorem 5.4, the LOT embedding can be used to separate 1s from 2s.

The data consisting of images of 1s and 2s is embedded in L^2 via the LOT embedding, where we choose as reference density σ an isotropic Gaussian as in the left plot of Figure 6. This means that every image μ (interpreted as a density on a grid $R \subset \mathbb{R}^2$) is assigned to the function $T_\sigma^\mu : \text{supp}(\sigma) \rightarrow R$. Since $\text{supp}(\sigma) \subset R$ is discrete, $T_\sigma^\mu(\text{supp}(\sigma))$ is a vector in \mathbb{R}^{2n} , where n is the number of grid points in $\text{supp}(\sigma)$. For each μ of the data set, we use this vector as input for the linear classification scheme (we use MATLAB’s “fitdiscr” function).

The experiment is conducted in the following way: We fix the number of testing data to 100 images from each class (i.e. in total, the testing data set consists of 200 images). Note that we only fix the number of testing data; the actual testing images are chosen randomly from the MNIST data set for each experiment. For the training data set we randomly choose N images from each class, where $N = 40, 60, 80, 100$. For each choice N , we run 5 experiments. In each experiment, the classification error of the test data is computed. Then the mean and standard deviation for every N is computed. The mean classification error is shown in Figure 7 as a function of N .

It is clear from the figure that the mean error decreases as the number of training data increases. Note however that we start with a very small amount of training data (40 images from each class), and test on 100 images from each class. The resulting mean error is only ≈ 0.13 . When we train on the same amount as we test (100 images per class), the mean error is already down to ≈ 0.02 .

The classification result is also visualized via LDA embedding plots in Figure 8 for two experiments. These plots again underline the fact that separation improves as the training data is increased. While training on 100 images per class (right plot of Figure 8) leads to almost perfect separation, training on 40 images per class (left plot of Figure 8) still performs very well considering the small size of the training set.

In addition to the fact that the LOT embedding is capable of producing good separation results on small training data, there is yet another benefit connected to the dimensionality of the problem. To run LDA (or any linear classifier), a matrix of data points versus features needs to be constructed. If we were to compare the original images, the feature space would have dimension equal

Classification of MNIST digits with LOT

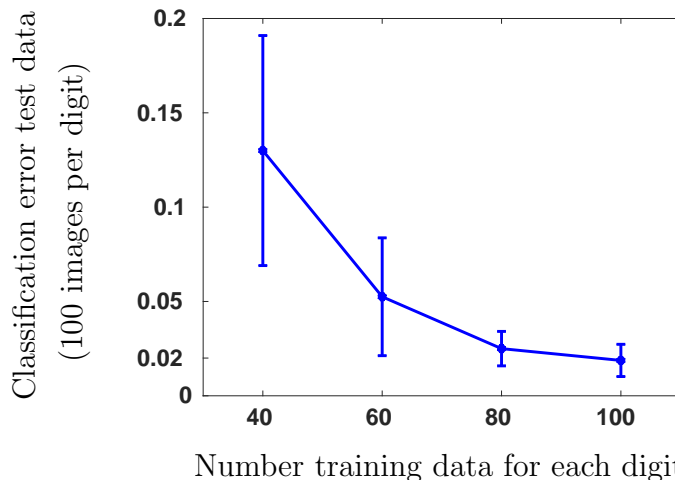


Figure 7: Classification of MNIST digits 1s and 2s with LOT embedding. We fix the number of testing data (100 images per digit), and vary the number of training data, $N = 40, 60, 80, 100$ (the actual training and testing sets are chosen randomly for each experiment). We train a linear classifier on the LOT embedding of the training data. The figure shows the mean and standard deviation of the classification error of the testing data over 5 experiments for each N .

to the number of grid points. In the LOT embedding only the grid points in $\text{supp}(\sigma)$ need to be considered, rather than the whole grid, which drastically reduces the dimension of the feature space. In the experiments we ran with MNIST, the grid is of size 28×28 , which leads to dimension $28^2 = 784$, while the support of σ is ≈ 70 grid points, hence the dimension is 140.

This dimension reduction allows us to run LDA on small training data as we did in these experiments. If the feature dimension is very high, one also needs a lot of training data to prevent zero within-class variance.

Acknowledgements

AC is supported by NSF DMS grants 1819222 and 2012266, and by Russell Sage Foundation Grant 2196.

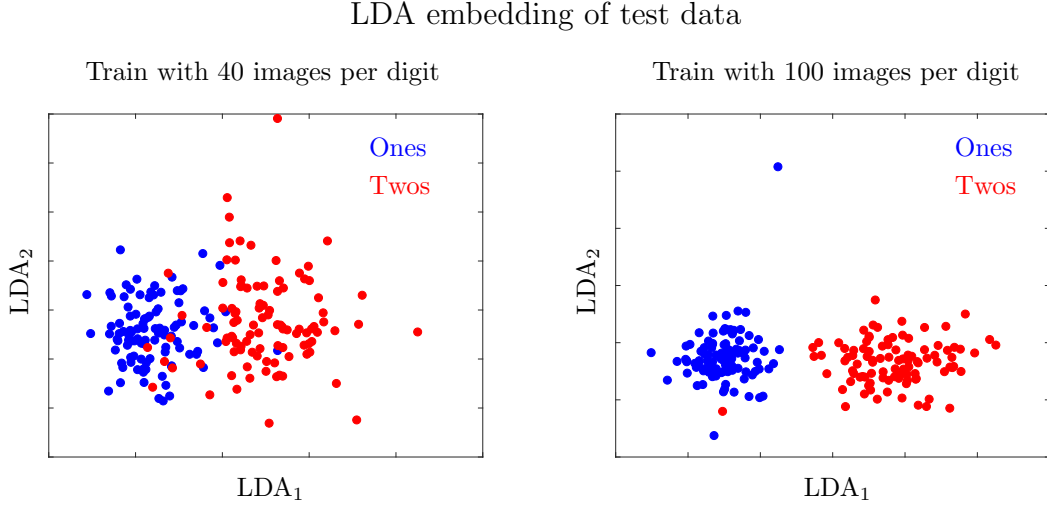


Figure 8: LDA embedding plots for the MNIST classification of digits 1 and 2 using LOT. As Figure 7, these plots underline that the classification improves with the amount of training data. *Left:* We choose one of the experiments carried out for $N = 40$ training data for each digit. The testing data (100 images per digit) is embedded in \mathbb{R}^2 through the LDA coordinates. The mean error (Figure 7) is ≈ 0.13 , which corresponds to ≈ 26 digits being misclassified. *Right:* We choose one of the experiments carried out for $N = 100$ training data for each digit. The testing data (100 images per digit) is embedded in \mathbb{R}^2 through the LDA coordinates. The mean error (Figure 7) is ≈ 0.15 , which corresponds to ≈ 3 digits being misclassified.

Appendix A Regularity of the LOT embedding

The main results of this paper are based on Hölder regularity-type properties of the LOT embedding, which are derived in this section.

One of the main ingredients is a version of a theorem on the regularity of the optimal transport map proved by L. A. Caffarelli [7, 8, 9]. The formulation of the theorem is taken from [13]:

Theorem A.1 (Caffarelli’s regularity theorem). *Let $\sigma, \mu \in \mathcal{P}_2(\mathbb{R}^n)$ with $\sigma, \mu \ll \lambda$. Assume that $\text{supp}(\sigma), \text{supp}(\mu)$ are C^2 and uniformly convex. Further assume that for some $\alpha \in (0, 1)$, the densities f_σ, f_μ are $C^{0,\alpha}$ continuous on their supports and assume that they are bounded from above and below, i.e. there exist constants $c, C, \bar{c}, \bar{C} > 0$ such that*

$$\begin{aligned} 0 < c &\leq \|f_\sigma\|_\infty \leq C, \\ 0 < \bar{c} &\leq \|f_\mu\|_\infty \leq \bar{C}. \end{aligned}$$

Then T_μ^σ is the gradient of a $C^{2,\alpha}$ function on $\text{supp}(\mu)$.

Definition A.2. We introduce the concept of k -strong convexity:

1. Let $f : X \rightarrow \mathbb{R}$ with $X \subseteq \mathbb{R}^n$ convex. f is called k -strongly convex if $g_k(x) = f(x) - \frac{1}{2}k\|x\|^2$ is convex.
2. For two measures $\sigma, \mu \in \mathcal{P}_2(\mathbb{R}^n)$ with $\text{supp}(\sigma)$ convex, denoted by K_σ^μ the supremum over all k such that φ with $\nabla\varphi = T_\sigma^\mu$, is k -strongly convex on $\text{supp}(\sigma)$.

In [13, Corollary 3.2] it is proved that if σ, μ satisfy the assumptions of Caffarelli's regularity theorem (Theorem A.1), then $K_\sigma^\mu > 0$. We further cite the following result from [13]:

Theorem A.3 ([13, Proposition 3.3]). Let $\sigma, \mu \in \mathcal{P}_2(\mathbb{R}^n)$ and assume they satisfy the same assumptions as in Caffarelli's regularity theorem (Theorem A.1). Then for every S that pushes σ to μ we have

$$\|S - T_\sigma^\mu\|_\sigma^2 \leq \frac{1}{K_\mu^\sigma} (\|S - \text{Id}\|_\sigma^2 - W_2(\sigma, \mu)^2).$$

Note that in the formulation of this theorem in [13], $2/K_\mu^\sigma$ appears instead of $1/K_\mu^\sigma$ in the bound. From the proof presented in [13] it can be seen, however, that 2 can be replaced by 1.

We now prove a bound on the LOT embedding. The proof is based on Theorem A.3 and [13, Corollary 3.4].

Theorem A.4. Let $\sigma, \nu_1, \nu_2 \in \mathcal{P}_2(\mathbb{R}^n)$, $\sigma, \nu_1, \nu_2 \ll \lambda$. Suppose that σ and ν_2 satisfy the assumptions of Caffarelli's regularity theorem (Theorem A.1). Then

$$\|F_\sigma(\nu_1) - F_\sigma(\nu_2)\|_\sigma \leq \left(\frac{2}{K_{\nu_2}^\sigma} + 1 \right) W_2(\nu_1, \nu_2) + 2 \left(\frac{W_2(\sigma, \nu_2)}{K_{\nu_2}^\sigma} \right)^{1/2} W_2(\nu_1, \nu_2)^{1/2}.$$

Proof. Let $S = T_{\nu_1}^{\nu_2}$. We aim at finding a bound on $\|T_\sigma^{\nu_1} - T_\sigma^{\nu_2}\|_\sigma$.

The triangle inequality and change-of-variables formula imply

$$\begin{aligned} \|S \circ T_\sigma^{\nu_1} - T_\sigma^{\nu_2}\|_\sigma &\geq \|T_\sigma^{\nu_1} - T_\sigma^{\nu_2}\|_\sigma - \|S \circ T_\sigma^{\nu_1} - T_\sigma^{\nu_1}\|_\sigma = \|T_\sigma^{\nu_1} - T_\sigma^{\nu_2}\|_\sigma - \|S - \text{Id}\|_{\nu_1} \\ &= \|T_\sigma^{\nu_1} - T_\sigma^{\nu_2}\|_\sigma - W_2(\nu_1, \nu_2). \end{aligned}$$

Thus we get

$$\|T_\sigma^{\nu_1} - T_\sigma^{\nu_2}\|_\sigma \leq \|S \circ T_\sigma^{\nu_1} - T_\sigma^{\nu_2}\|_\sigma + W_2(\nu_1, \nu_2) \quad (17)$$

Theorem A.3 implies

$$\|S \circ T_\sigma^{\nu_1} - T_\sigma^{\nu_2}\|_\sigma^2 \leq \frac{1}{K_{\nu_2}^\sigma} (\|S \circ T_\sigma^{\nu_1} - \text{Id}\|_\sigma^2 - W_2(\sigma, \nu_2)^2). \quad (18)$$

Again by the triangle inequality and the change-of-variables formula we have

$$\begin{aligned} \|S \circ T_\sigma^{\nu_1} - \text{Id}\|_\sigma &\leq \|S \circ T_\sigma^{\nu_1} - T_\sigma^{\nu_1}\|_\sigma + \|T_\sigma^{\nu_1} - \text{Id}\|_\sigma = W_2(\nu_1, \nu_2) + W_2(\sigma, \nu_1) \\ &\leq 2W_2(\nu_1, \nu_2) + W_2(\sigma, \nu_2) \end{aligned}$$

Combining this with (18) we obtain

$$\|S \circ T_{\sigma}^{\nu_1} - T_{\sigma}^{\nu_2}\|_{\sigma}^2 \leq \frac{4}{K_{\nu_2}^{\sigma}} (W_2(\nu_1, \nu_2)^2 + W_2(\nu_1, \nu_2)W_2(\sigma, \nu_2)).$$

Taking the square root and using the fact that $(a+b)^{1/2} \leq a^{1/2} + b^{1/2}$ we obtain

$$\|S \circ T_{\sigma}^{\nu_1} - T_{\sigma}^{\nu_2}\|_{\sigma} \leq \frac{2}{K_{\nu_2}^{\sigma^{1/2}}} (W_2(\nu_1, \nu_2) + (W_2(\nu_1, \nu_2)W_2(\sigma, \nu_2))^{1/2}).$$

Now (17) implies the result. \square

Note that the “constants” in Theorem A.4 depend on ν_2 (namely $K_{\nu_2}^{\sigma}$ and $W_2(\sigma, \nu_2)$). This can be avoided by considering $\nu_2 \in \mathcal{E} \star \mu$ for a fixed $\mu \in \mathcal{P}_2(\mathbb{R}^n)$, where \mathcal{E} denotes the set of shifts and scalings. As a preparation for this result, we need the following lemma:

Lemma A.5. *Let $f : X \rightarrow \mathbb{R}$ be differentiable with $X \subseteq \mathbb{R}^n$ convex. Then we have the following:*

1. *f is k -strongly convex on X if and only if $f \circ S_a$ is k -strongly convex on $S_a^{-1}(X)$.*
2. *f is k -strongly convex on X if and only if $R_c^{-1} \circ f \circ R_c$ is (kc) -strongly convex on $R_c^{-1}(X)$.*

Proof. We first note that X is convex if and only if $h^{-1}(X)$ is convex for $h = S_a$ or $h = R_c$. Furthermore, f is k -strongly convex if and only if

$$(\nabla f(x) - \nabla f(y))^T(x - y) \geq k\|x - y\|^2, \quad x, y \in X. \quad (19)$$

For $\bar{x}, \bar{y} \in S_a^{-1}(X)$, eq. (19) implies that $f \circ S_a$ is k -strongly convex if and only if

$$(\nabla f \circ S_a(\bar{x}) - \nabla f \circ S_a(\bar{y}))^T(\bar{x} - \bar{y}) \geq k\|\bar{x} - \bar{y}\|^2$$

which is the same as

$$(\nabla f(S_a(\bar{x})) - \nabla f(S_a(\bar{y})))^T(S_a(\bar{x}) - S_a(\bar{y})) \geq k\|S_a(\bar{x}) - S_a(\bar{y})\|^2.$$

As this is only a transformation $x = S_a(\bar{x})$ and $y = S_a(\bar{y})$ compared to eq. (19), k -strong convexity of f and $f \circ S_a$ are equivalent.

For $\bar{x}, \bar{y} \in R_c^{-1}(X)$, eq. (19) implies that $R_c^{-1} \circ f \circ R_c$ is (kc) -strongly convex if and only if

$$(\nabla(R_c^{-1} \circ f \circ R_c)(\bar{x}) - \nabla(R_c^{-1} \circ f \circ R_c)(\bar{y}))^T(\bar{x} - \bar{y}) \geq kc\|\bar{x} - \bar{y}\|^2$$

which is the same as

$$c^{-1}(\nabla f(R_c(\bar{x})) - \nabla f(R_c(\bar{y})))^T(R_c(\bar{x}) - R_c(\bar{y})) \geq kc c^{-2}\|R_c(\bar{x}) - R_c(\bar{y})\|^2$$

resulting in

$$(\nabla f(R_c(\bar{x})) - \nabla f(R_c(\bar{y})))^T (R_c(\bar{x}) - R_c(\bar{y})) \geq k \|R_c(\bar{x}) - R_c(\bar{y})\|^2$$

As this is only a transformation $x = R_c(\bar{x})$ and $y = R_c(\bar{y})$ compared to eq. (19), k -strong convexity of f and (kc) -strong convexity of $R_c^{-1} \circ f \circ R_c$ are equivalent. \square

Corollary A.6. *Let $\sigma, \mu \in \mathcal{P}_2(\mathbb{R}^n)$, $\sigma, \mu \ll \lambda$. Further assume that σ and μ satisfy the assumptions of Caffarelli's regularity theorem (Theorem A.1). Let $R > 0$ and consider $h \in \mathcal{E}_{\mu, R}$ (bounded shifts/scalings, see eq. (13)) as well as $g \in L^2(\mathbb{R}^n, \mu)$. Then we have*

$$\begin{aligned} \|F_\sigma(g_\# \mu) - F_\sigma(h_\# \mu)\|_\sigma &\leq \left(\sqrt{\frac{4R}{K_\mu^\sigma}} + 1 \right) W_2(g_\# \mu, h_\# \mu) \\ &\quad + \left(4R \frac{W_2(\sigma, \mu) + R + \|\text{Id}\|_\mu}{K_\mu^\sigma} \right)^{1/2} W_2(g_\# \mu, h_\# \mu)^{1/2}. \end{aligned}$$

Note that we now have a bound with constants that do not depend on h or g . They only depend on the fixed measures σ, μ and on the radius R .

Proof. Let $\nu_1 = g_\# \mu$ and $\nu_2 = h_\# \mu$. First note that since μ and σ satisfy the assumptions of Caffarelli's regularity theorem, also ν_2 and σ satisfy them. Therefore we can apply Theorem A.4.

We now bound $W_2(\sigma, \nu_2)$ and $K_{\nu_2}^\sigma$ from Theorem A.4 by constants that only depend on σ, μ and R . Such bounds then imply the result.

The triangle inequality, Lemma 3.4 and the assumption $\|h\|_\mu < R$ imply

$$\begin{aligned} W_2(\sigma, \nu_2) &\leq W_2(\sigma, \mu) + W_2(\mu, h_\# \mu) = W_2(\sigma, \mu) + \|T_\mu^{h_\# \mu} - \text{Id}\|_\mu \\ &= W_2(\sigma, \mu) + \|h - \text{Id}\|_\mu \\ &< W_2(\sigma, \mu) + R + \|\text{Id}\|_\mu. \end{aligned}$$

We now show that $K_{\nu_2}^\sigma$ only depends on σ, μ and R , but does not depend on h . First consider $h = S_a$. Note that $T_{\nu_2}^\sigma = T_\mu^\sigma \circ S_a^{-1}$ and $T_\mu^\sigma = \nabla \psi$ implies $T_\mu^\sigma \circ S_a^{-1} = \nabla \psi \circ S_a^{-1}$. Also, $\psi \circ S_a^{-1}$ is convex on $S_a(\text{supp}(\mu))$. This implies that $\varphi = \psi \circ S_a^{-1}$.

Lemma A.5 implies that ψ is k -strongly convex if and only if $\varphi = \psi \circ S_a^{-1}$ is k -strongly convex. Therefore the modulus of uniform convexity of $\psi \circ S_a^{-1}$ equals the modulus of uniform convexity of ψ . Thus $K_{\nu_2}^\sigma = K_\mu^\sigma$, which is independent of S_a .

Now consider $h = R_c$. Again we have $T_{\nu_2}^\sigma = T_\mu^\sigma \circ R_c^{-1}$ and $T_\mu^\sigma = \nabla \psi$ implies $T_\mu^\sigma \circ R_c^{-1} = \nabla R_c \circ \psi \circ R_c^{-1}$. Also, $R_c \circ \psi \circ R_c^{-1}$ is convex on $R_c(\text{supp}(\mu))$. This implies that $\varphi = R_c \circ \psi \circ R_c^{-1}$.

Lemma A.5 implies that ψ is k -strongly convex if and only if $\varphi = R_c \circ \psi \circ R_c^{-1}$ is kc^{-1} -strongly convex. Therefore $K_{\nu_2}^\sigma = K_\mu^\sigma c^{-1}$. Since by assumption $|c| = \|R_c\|_\mu < R$ we have

$$\frac{1}{K_{\nu_2}^\sigma} = \frac{1}{K_\mu^\sigma} |c| < \frac{R}{K_\mu^\sigma},$$

which gives a bound independent of R_c . \square

We now combine Corollary A.6 with the Lipschitz continuity of the pushforward map $g \mapsto g_\# \sigma$ to obtain a Hölder regularity-type result for LOT. We first cite the result on the Lipschitz continuity of the pushforward map, which can be found in e.g. [3, Equation (2.1)]:

$$W_2(g_\# \mu, h_\# \mu) \leq \|g - h\|_\mu. \quad (20)$$

Corollary A.7. *Let $\sigma, \mu \in \mathcal{P}_2(\mathbb{R}^n)$, $\sigma, \mu \ll \lambda$. Further assume that σ and μ satisfy the assumptions of Caffarelli's regularity theorem (Theorem A.1). Let $R > 0$, $h \in \mathcal{E}_{\mu, R}$ (see eq. (13)) and $g \in L^2(\mathbb{R}^n, \mu)$. Then we have*

$$\begin{aligned} \|F_\sigma(g_\# \mu) - F_\sigma(h_\# \mu)\|_\sigma &\leq \left(\sqrt{\frac{4R}{K_\mu^\sigma}} + 1 \right) \|g - h\|_\mu \\ &\quad + \sqrt{4R \frac{W_2(\sigma, \mu) + R + \|\text{Id}\|_\mu}{K_\mu^\sigma}} \|g - h\|_\mu^{1/2}. \end{aligned}$$

Remark A.8. *In [13, Corollary 3.4] it is proved that for fixed σ and a Lipschitz continuous curve μ_t of absolutely continuous measures, $t \in [0, 1]$, $1/2$ -Hölder regularity of $t \mapsto F_\sigma(\mu_t)$ can be achieved. Indeed, it is proved that*

$$\|F_\sigma(\mu_t) - F_\sigma(\mu_0)\|_\sigma \leq C\sqrt{t}.$$

Corollary A.7 can be considered a generalization of this result. We prove that the map $h \mapsto F_\sigma(h_\# \mu)$ can achieve Hölder-type regularity between an element of \mathcal{E} (comparable to μ_0) and an element of $L^2(\mathbb{R}^n, \mu)$ (comparable to μ_t). Note that like μ_t , the “curve” $h \mapsto h_\# \mu$ is Lipschitz continuous (eq. (20)). The restriction to bounded shifts and scalings (via $R > 0$) relates to the fact that $[0, 1]$ is bounded.

Appendix B Set-up for linear separability results

In this section we build up the theory needed for the results on linear separability presented in Section 5. The proofs for these results can then be derived easily from results of this section, see Section E.

Throughout this section, let $\mathcal{H} \subseteq L^2(\mathbb{R}^n, \sigma)$. Then \mathcal{H} acts on $\mathcal{P}_2(\mathbb{R}^n)$ by push-forward

$$h \star \mu = h_\# \mu, \quad h \in \mathcal{H}, \mu \in \mathcal{P}_2(\mathbb{R}^n).$$

This is a group action if \mathcal{H} is a subgroup of $L^2(\mathbb{R}^n, \sigma)$.

Fix $\mu \in \mathcal{P}_2(\mathbb{R}^n)$. Using the notation from Theorem 4.3, we denote by

$$\mathcal{H} \star \mu = \{h \star \mu : h \in \mathcal{H}\}$$

the orbit of μ with respect to the action of \mathcal{H} .

Note that \mathcal{H} also acts on $L^2(\mathbb{R}^n, \sigma)$ by composition, i.e. $h \star f = h \circ f$ for $f \in L^2(\mathbb{R}^n, \sigma)$ and $h \in \mathcal{H}$. We also denote this action by \star .

We now derive some properties of this action in connection with the LOT embedding F_σ .

Definition B.1. Let $\sigma, \mu \in \mathcal{P}_2(\mathbb{R}^n)$, $\sigma \ll \lambda$, and let $\mathcal{H} \subseteq L^2(\mathbb{R}^n, \sigma)$. We say that F_σ is compatible with μ -orbits with respect to the action of \mathcal{H} if

$$F_\sigma(h \star \mu) = h \star F_\sigma(\mu), \quad h \in \mathcal{H}. \quad (21)$$

Remark B.2. Note that Equation (21) is exactly eq. (8). We just introduced a new notation via \star .

As is shown in Lemma 3.4, Condition (21) is satisfied by shifts and scalings in arbitrary dimension, and by all monotonically increasing functions in dimension $n = 1$.

Lemma B.3. Let $\sigma, \mu \in \mathcal{P}_2(\mathbb{R}^n)$, $\sigma \ll \lambda$, and let $\mathcal{H} \subseteq L^2(\mathbb{R}^n, \sigma)$ be convex. If F_σ is compatible with μ -orbits with respect to the action of \mathcal{H} (Definition B.1) then $F_\sigma(\mathcal{H} \star \mu)$ is convex.

Proof. We prove that for $f \in L^2(\mathbb{R}^n, \sigma)$, convexity of \mathcal{H} implies convexity of $\mathcal{H} \star f$. This together with condition (21) then implies convexity of $F_\sigma(\mathcal{H} \star \mu)$.

Let $c \in [0, 1]$ and let $h_1, h_2 \in \mathcal{H}$. Then

$$(1 - c)(h_1 \circ f) + c(h_2 \circ f) = ((1 - c)h_1 + ch_2) \circ f \in \mathcal{H} \star f. \quad \square$$

Theorem B.4. Let $\sigma, \mu, \nu \in \mathcal{P}_2(\mathbb{R}^n)$, $\sigma \ll \lambda$ and let $\mathcal{H} \subseteq L^2(\mathbb{R}^n, \sigma)$ be convex. Further assume that F_σ is compatible with both μ - and ν -orbits with respect to the action of \mathcal{H} (Definition B.1). If $\mathcal{H} \star \mu$ is closed and $\mathcal{H} \star \nu$ is compact, and these two sets are disjoint, then $F_\sigma(\mathcal{H} \star \mu)$ and $F_\sigma(\mathcal{H} \star \nu)$ are linearly separable.

Proof. Since F_σ is continuous, $F_\sigma(\mathcal{H} \star \mu)$ is compact and $F_\sigma(\mathcal{H} \star \nu)$ is closed. Since F_σ is injective (Lemma 3.2), they are also disjoint. Lemma B.3 implies that both images are convex. Therefore, the Hahn-Banach Theorem implies separability. \square

Definition B.1 is a strong condition which is satisfied for shifts and scalings. In the following we show a linear separability result which relaxes this condition. Indeed, we show that Theorem B.4 is also true if we extend \mathcal{H} by functions which are ε -close to shifts and scalings in $L^2(\mathbb{R}^n, \sigma)$. In analogy to Definition B.1 we define compatibility of F_σ with respect to μ -orbits up to an error ε .

Definition B.5. Let $\sigma, \mu \in \mathcal{P}_2(\mathbb{R}^n)$, $\sigma \ll \lambda$, let $\mathcal{H} \subseteq L^2(\mathbb{R}^n, \sigma)$, and let $\varepsilon > 0$. We say that F_σ is ε -compatible with μ -orbits with respect to the action of \mathcal{H} if

$$\|F_\sigma(h \star \mu) - h \star F_\sigma(\mu)\|_\sigma < \varepsilon \quad h \in \mathcal{H}.$$

There is also an analog to Lemma B.3:

Lemma B.6. Let $\sigma, \mu \in \mathcal{P}_2(\mathbb{R}^n)$, $\sigma \ll \lambda$, let $\mathcal{H} \subseteq L^2(\mathbb{R}^n, \sigma)$ be convex, and let $\varepsilon > 0$. If F_σ is ε -compatible with μ -orbits with respect to the action of \mathcal{H} (Definition B.5) then $F_\sigma(\mathcal{H} \star \mu)$ is 2ε -convex (Definition F.1).

Proof. Let $h_1, h_2 \in \mathcal{H}$ and $c \in [0, 1]$. Define $h = (1 - c)h_1 + ch_2 \in \mathcal{H}$. We aim at proving that

$$\|(1 - c)F_\sigma(h_1 \star \mu) + cF_\sigma(h_2 \star \mu) - F_\sigma(h \star \mu)\|_\sigma < 2\varepsilon.$$

To this end, we apply Definition B.5:

$$\begin{aligned} & \|(1 - c)F_\sigma(h_1 \star \mu) + cF_\sigma(h_2 \star \mu) - F_\sigma(h \star \mu)\|_\sigma \leq \\ & (1 - c)\|F_\sigma(h_1 \star \mu) - h_1 \star F_\sigma(\mu)\|_\sigma + c\|F_\sigma(h_2 \star \mu) - h_2 \star F_\sigma(\mu)\|_\sigma \\ & \quad + \|h \star F_\sigma(\mu) - F_\sigma(h \star \mu)\|_\sigma \\ & < (1 - c)\varepsilon + c\varepsilon + \varepsilon = 2\varepsilon. \end{aligned} \quad \square$$

This lemma allows us to establish the most general form of the linear separability theorem, which simply requires the additional assumption that the two families generated by action \mathcal{H} , $\mathcal{H} \star \mu$ and $\mathcal{H} \star \nu$, have a minimal distance greater than 6ε .

Theorem B.7. *Let $\sigma, \mu, \nu \in \mathcal{P}_2(\mathbb{R}^n)$, $\sigma \ll \lambda$, let $\mathcal{H} \subseteq L^2(\mathbb{R}^n, \sigma)$ be convex, and let $\varepsilon > 0$. Further assume that F_σ is ε -compatible with both μ - and ν -orbits with respect to the action of \mathcal{H} (Definition B.5). If $\mathcal{H} \star \mu$ and $\mathcal{H} \star \nu$ are compact, and $W_2(h_1 \star \mu, h_2 \star \nu) > 6\varepsilon$ for all $h_1, h_2 \in \mathcal{H}$, then $F_\sigma(\mathcal{H} \star \mu)$ and $F_\sigma(\mathcal{H} \star \nu)$ are linearly separable.*

Proof. Since F_σ is continuous, both $A = F_\sigma(\mathcal{H} \star \mu)$ and $B = F_\sigma(\mathcal{H} \star \nu)$ are compact. Now consider the closed convex hull of these sets, i.e. consider $\text{conv}(A)$ and $\text{conv}(B)$. The closed convex hull of compact sets is compact again in a completely metrizable locally convex space [2, Theorem 5.35]. Thus, in order to apply the Hahn-Banach theorem to $\text{conv}(A)$ and $\text{conv}(B)$, we only need to show that these sets are disjoint.

Theorem 4.1 implies

$$6\varepsilon < W_2(h_1 \star \mu, h_2 \star \nu) \leq \|F_\sigma(h_1 \star \mu) - F_\sigma(h_2 \star \nu)\|_\sigma,$$

for $h_1, h_2 \in \mathcal{H}$. Therefore $d(A, B) > 6\varepsilon$, where d denotes the distance between sets.

Since F_σ is ε -compatible with respect to both μ - and ν -orbits, Lemma B.6 implies that both A and B are 2ε -convex (Definition F.1). This means that $d(\text{conv}(A), A) < 2\varepsilon$ and $d(\text{conv}(B), B) < 2\varepsilon$.

Lemma F.2 now implies that $d(\text{conv}(A), \text{conv}(B)) > \varepsilon$. Therefore the closure of these sets has positive distance, $d(\text{conv}(A), \text{conv}(B)) > 0$, which implies that $\text{conv}(A) \cap \text{conv}(B) = \emptyset$. \square

Appendix C Proofs of Section 3

Proof of Lemma 3.2. To prove part 1 of the lemma, we show continuity and injectivity of F_σ .

The stability of transport maps as described in [29, Corollary 5.23] implies that F_σ is continuous.

If $F_\sigma(\nu_1) = F_\sigma(\nu_2)$, then $T_\sigma^{\nu_1} = T_\sigma^{\nu_2}$. In particular this implies

$$\nu_1 = T_\sigma^{\nu_1} \# \sigma = T_\sigma^{\nu_2} \# \sigma = \nu_2.$$

This implies injectivity of F_σ .

To prove part 2 of the lemma, let $c \in [0, 1]$ and let $\nu_1, \nu_2 \in \mathcal{P}_2(\mathbb{R}^n)$. We define

$$T(x) := (1 - c) F_\sigma(\nu_1)(x) + c F_\sigma(\nu_2)(x), \quad x \in \mathbb{R}^n.$$

We need to show that there exists $\nu_3 \in \mathcal{P}_2(\mathbb{R}^n)$ such that $T = F_\sigma(\nu_3)$. To this end, we define $\nu_3 := T_\# \sigma$. By definition, T pushes σ to ν_3 . We now show that T can be written as the gradient of a convex function.

By Theorem 2.1 there exist convex functions φ_1, φ_2 such that $T_\sigma^{\nu_1}$ and $T_\sigma^{\nu_2}$ can be written uniquely as $T_\sigma^{\nu_j}(x) = \nabla \varphi_j(x)$, $j = 1, 2, x \in \mathbb{R}^n$. This implies that $T(x) = \nabla \varphi_3(x)$, with the convex function

$$\varphi_3(x) = (1 - c) \varphi_1(x) + c \varphi_2(x), \quad x \in \mathbb{R}^n.$$

Theorem 2.1 thus implies that $T = T_\sigma^{\nu_3}$, which proves $T = F_\sigma(\nu_3)$. \square

Proof of Lemma 3.4. On \mathbb{R} recall that

$$T_\sigma^\nu = G_\nu^{-1} \circ G_\sigma, \quad (22)$$

where G_σ denotes the cdf of σ defined by $G_\sigma(x) = \sigma((-\infty, x])$. Now if h is monotonically increasing, we have $G_{h\# \mu} = G_\mu \circ h^{-1}$, which implies compatibility.

Let $n \geq 1$ and $h \in \mathcal{E}$. We first consider the case $h = S_a$ for some $a \in \mathbb{R}^n$. By Theorem 2.1, both T_σ^ν and $T_\sigma^{S_a\# \nu}$ exist. We now prove $T_\sigma^{S_a\# \nu} = S_a \circ T_\sigma^\nu$, which shows the result for $h = S_a$.

Again, by Theorem 2.1, there exists a unique convex function φ such that $T_\sigma^\nu = \nabla \varphi$. Then

$$(S_a \circ T_\sigma^\nu)(x) = \nabla \varphi(x) + a = \nabla (\varphi(x) + \langle a, x \rangle) = \nabla \psi(x),$$

where ψ is also convex.

Due to the general property

$$(\tilde{T} \circ T)_\# \sigma = \tilde{T}_\# (T_\# \sigma) \quad (23)$$

for maps T, \tilde{T} , we have that $S_a \circ T_\sigma^\nu$ pushes σ to $S_{a\#} \nu$. Therefore Theorem 2.1 implies that $S_a \circ T_\sigma^\nu = T_\sigma^{S_a\# \nu}$.

We now consider the case $h = R_c$ for some $c \in \mathbb{R}$. By Theorem 2.1, both T_σ^ν and $T_\sigma^{R_c\# \nu}$ exist. We now prove that $T_\sigma^{R_c\# \nu} = R_c \circ T_\sigma^\nu$, which implies the result for $h = R_c$.

Again, by Theorem 2.1, there exists a unique convex function φ such that $T_\sigma^\nu = \nabla \varphi$. Then

$$(R_c \circ T_\sigma^\nu)(x) = c \nabla \varphi(x) = \nabla c \varphi(x) = \nabla \psi(x),$$

where ψ is also convex. Furthermore, by eq. (23), $R_c \circ T_\sigma^\nu$ pushes σ to $R_{c\#} \nu$. Therefore Theorem 2.1 implies $T_\sigma^{R_c\# \nu} = R_c \circ T_\sigma^\nu$. \square

Appendix D Proofs of Section 4

Lemma D.1. Fix $\sigma, \mu \in \mathcal{P}_2(\mathbb{R}^n)$, $\sigma \ll \lambda$. If F_σ is compatible with μ -pushforwards of a set of functions $\mathcal{H} \subseteq L^2(\mathbb{R}^n, \mu)$ (see eq. (8)) then for $h_1, h_2 \in \mathcal{H}$ we have

$$T_{h_1 \# \mu}^{h_2 \# \mu} = T_\sigma^{h_2 \# \mu} \circ T_{h_2 \# \mu}^\sigma.$$

Proof. Denote by $\nu_1 = h_1 \# \mu, \nu_2 = h_2 \# \mu$. Compatibility (eq. (8)) implies

$$T_\sigma^{\nu_j} = h_j \circ T_\sigma^\mu, \quad j = 1, 2. \quad (24)$$

This implies

$$T_\sigma^{\nu_2} \circ T_{\nu_1}^\sigma = h_2 \circ T_\sigma^\mu \circ (h_1 \circ T_\sigma^\mu)^{-1} = h_2 \circ h_1^{-1}.$$

Again by eq. (8), we obtain

$$T_{\nu_1}^{\nu_2} = h_2 \circ T_{\nu_1}^\mu = h_2 \circ (T_\mu^{\nu_1})^{-1} = h_2 \circ (h_1 \circ T_\mu^\mu)^{-1} = h_2 \circ h_1^{-1}. \quad \square$$

Proof of Theorem 4.4. Since $g_1, g_2 \in \mathcal{G}_{\mu, R, \varepsilon}$ there exist $h_1, h_2 \in \mathcal{E}_{\mu, R}$ such that $\|g_1 - h_1\|_\mu < \varepsilon$ and $\|g_2 - h_2\|_\mu < \varepsilon$. The triangle inequality implies

$$\begin{aligned} \|F_\sigma(g_1 \# \mu) - F_\sigma(g_2 \# \mu)\|_\sigma &\leq \|F_\sigma(g_1 \# \mu) - F_\sigma(h_1 \# \mu)\|_\sigma \\ &\quad + \|F_\sigma(h_1 \# \mu) - F_\sigma(h_2 \# \mu)\|_\sigma + \|F_\sigma(h_2 \# \mu) - F_\sigma(g_2 \# \mu)\|_\sigma \end{aligned} \quad (25)$$

Corollary A.7 implies that there exist constants $C_{\sigma, \mu, R}, \overline{C}_{\sigma, \mu, R}$ such that

$$\begin{aligned} \|F_\sigma(g_i \# \mu) - F_\sigma(h_i \# \mu)\|_\sigma &\leq C_{\sigma, \mu, R} \|g_i - h_i\|_\mu + \overline{C}_{\sigma, \mu, R} \|g_i - h_i\|_\mu^{1/2} \\ &\leq C_{\sigma, \mu, R} \varepsilon + \overline{C}_{\sigma, \mu, R} \varepsilon^{1/2}, \end{aligned} \quad (26)$$

for $i = 1, 2$. Note that the same constants can be used for $i = 1$ and $i = 2$ since R bounds both h_1 and h_2 .

Theorem 4.3, eq. (20) and the triangle inequality imply

$$\begin{aligned} \|F_\sigma(h_1 \# \mu) - F_\sigma(h_2 \# \mu)\|_\sigma &= W_2(h_1 \# \mu, h_2 \# \mu) \\ &\leq W_2(h_1 \# \mu, g_1 \# \mu) + W_2(g_1 \# \mu, g_2 \# \mu) + W_2(g_2 \# \mu, h_2 \# \mu) \\ &\leq \|h_1 - g_1\|_\mu + W_2(g_1 \# \mu, g_2 \# \mu) + \|g_2 - h_2\|_\mu \\ &\leq 2\varepsilon + W_2(g_1 \# \mu, g_2 \# \mu). \end{aligned}$$

Using this inequality as well as eq. (26) in eq. (25) we obtain

$$\|F_\sigma(g_1 \# \mu) - F_\sigma(g_2 \# \mu)\|_\sigma \leq 2(C_{\sigma, \mu, R} + 1) \varepsilon + 2\overline{C}_{\sigma, \mu, R} \varepsilon^{1/2} + W_2(g_1 \# \mu, g_2 \# \mu),$$

which concludes the proof. \square

Appendix E Proofs of Section 5

Proof of Theorems 5.1 and 5.3. By Remark B.2, the compatibility condition (21) is satisfied. Thus we can apply Theorem B.4. \square

Proof of Theorem 5.4. We show that F_σ is δ -compatible with both μ - and ν -orbits with respect to the action of \mathcal{G} . Then the result follows from Theorem B.7.

Let $g \in \mathcal{G}$ and $h \in \mathcal{E}_{\lambda,R}$ such that $\|g - h\| \leq \varepsilon$. Since $h \in \mathcal{E}_{\lambda,R}$ it is compatible with μ -orbits. First note that

$$\|h \star F_\sigma(\mu) - g \star F_\sigma(\mu)\|_\sigma = \|h \circ T_\sigma^\mu - g \circ T_\sigma^\mu\|_\sigma = \|h - g\|_\mu \leq \|f_\mu\|_\infty^{1/2} \varepsilon$$

This estimate, together with Corollary A.7 implies

$$\begin{aligned} \|F_\sigma(g \star \mu) - g \star F_\sigma(\mu)\|_\sigma &\leq \|F_\sigma(g \star \mu) - F_\sigma(h \star \mu)\|_\sigma + \|h \star F_\sigma(\mu) - g \star F_\sigma(\mu)\|_\sigma \\ &\leq \delta. \end{aligned}$$

Similarly, it can be shown that F_σ is δ -compatible with ν -orbits. \square

Appendix F A useful result in normed spaces

In this section we derive a result on almost convex sets for general normed spaces. It states that if two almost convex sets are separated by a positive value, then their convex hull can also be separated.

This result is needed for the almost linear separability proof for perturbed shifts and scalings (Theorems B.7 and 5.4).

Definition F.1. Let $(X, \|\cdot\|)$ be a normed space and let $\varepsilon > 0$. X is called ε -convex if for every $x_1, x_2 \in X$ and $c \in [0, 1]$ there exists $x \in X$ such that

$$\|(1 - c)x_1 + cx_2 - x\| < \varepsilon.$$

This definition states that for an ε -convex set X , $d(\text{conv}(X), X) < \varepsilon$, where $\text{conv}(X)$ denotes the convex hull of X and d is the distance between sets.

Lemma F.2. Let $(X, \|\cdot\|)$ be a normed space and let $\varepsilon > 0$. Consider two ε -convex sets $A, B \subset X$. If $d(A, B) > 3\varepsilon$, then $d(\text{conv}(A), \text{conv}(B)) > \varepsilon$.

Proof. Let $a \in A$ and $c_b \in \text{conv}(B)$. Let $b \in B$ such that $\|c_b - b\| < \varepsilon$. Then

$$\|a - c_b\| \geq \|a - b\| - \|b - c_b\| > 3\varepsilon - \varepsilon = 2\varepsilon.$$

Therefore $d(A, \text{conv}(B)) > 2\varepsilon$. Similarly one can prove that $d(B, \text{conv}(A)) > 2\varepsilon$.

Now let $c_a \in \text{conv}(A)$ and $c_b \in \text{conv}(B)$ and choose $b \in B$ such that $\|c_b - b\| < \varepsilon$. Then we have

$$\|c_a - c_b\| \geq \|c_a - b\| - \|b - c_b\| > 2\varepsilon - \varepsilon = \varepsilon,$$

which implies that $d(\text{conv}(A), \text{conv}(B)) > \varepsilon$. \square

References

- [1] A. ALDROUBI, S. LI, AND G. K. ROHDE, *Partitioning signal classes using transport transforms for data analysis and machine learning*. <https://arxiv.org/abs/2008.03452>, 2020.
- [2] C. D. ALIPRANTIS AND K. C. BORDER, *Infinite Dimensional Analysis: A Hitchhiker’s Guide*, Springer, Berlin; London, 2006.
- [3] L. AMBROSIO AND N. GIGLI, *A User’s Guide to Optimal Transport*, Springer Berlin Heidelberg, Berlin, Heidelberg, 2013, pp. 1–155.
- [4] M. ARJOVSKY, S. CHINTALA, AND L. BOTTOU, *Wasserstein generative adversarial networks*, in Proceedings of Machine Learning Research, D. Precup and Y. W. Teh, eds., vol. 70, PMLR, 2017, pp. 214–223.
- [5] Y. BRENIER, *Polar factorization and monotone rearrangement of vector-valued functions*, Comm. Pure Appl. Math., 44 (1991), pp. 375–417.
- [6] R. V. BRUGGNER, B. BODENMILLER, D. L. DILL, R. J. TIBSHIRANI, AND G. P. NOLAN, *Automated identification of stratifying signatures in cellular subpopulations*, Proceedings of the National Academy of Sciences, 111 (2014), pp. E2770–E2777.
- [7] L. A. CAFFARELLI, *Boundary regularity of maps with convex potentials*, Communications on Pure and Applied Mathematics, 45 (1992), pp. 1141–1151.
- [8] ———, *The regularity of mappings with a convex potential*, Journal of the American Mathematical Society, 5 (1992), pp. 99–104.
- [9] ———, *Boundary regularity of maps with convex potentials–II*, Annals of Mathematics, 144 (1996), pp. 453–496.
- [10] X. CHENG, A. CLONINGER, AND R. R. COIFMAN, *Two-sample statistics based on anisotropic kernels*, Information and Inference: A Journal of the IMA, (2017).
- [11] A. CLONINGER, B. ROY, C. RILEY, AND H. M. KRUMHOLZ, *People mover’s distance: Class level geometry using fast pairwise data adaptive transportation costs*, Applied and Computational Harmonic Analysis, 47 (2019), pp. 248–257.
- [12] M. CUTURI, *Sinkhorn distances: Lightspeed computation of optimal transport*, in Advances in neural information processing systems, 2013, pp. 2292–2300.
- [13] N. GIGLI, *On Hölder continuity-in-time of the optimal transport map towards measures along a curve*, Proceedings of the Edinburgh Mathematical Society, 54 (2011), p. 401–409.

- [14] S. KOLOURI, S. R. PARK, AND G. K. ROHDE, *The radon cumulative distribution transform and its application to image classification*, IEEE Transactions on Image Processing, 25 (2016), pp. 920–934.
- [15] Y. LECUN AND C. CORTES, *The MNIST database of handwritten digits*. <http://yann.lecun.com/exdb/mnist/>, 1998.
- [16] W. LEEB AND R. COIFMAN, *Hoelder-lipschitz norms and their duals on spaces with semigroups, with applications to earth mover’s distance*, Journal of Fourier Analysis and Applications, 22 (2016), pp. 910–953.
- [17] G. LOEPER, *On the regularity of the polar factorization for time dependent maps*, Calc. Var., 22 (2005), pp. 343–374.
- [18] R. J. MCCANN, *Polar factorization of maps on Riemannian manifolds*, Geometric & Functional Analysis GAFA, 11 (2001), pp. 589–608.
- [19] G. MISHNE, R. TALMON, R. MEIR, J. SCHILLER, M. LAVZIN, U. DUBIN, AND R. R. COIFMAN, *Hierarchical coupled-geometry analysis for neuronal structure and activity pattern discovery*, IEEE Journal of Selected Topics in Signal Processing, 10 (2016), pp. 1238–1253.
- [20] K. MUANDET, K. FUKUMIZU, B. SRIPERUMBUDUR, AND B. SCHÖLKOPF, *Kernel Mean Embedding of Distributions: A Review and Beyond*, Now Foundations and Trends, 2017.
- [21] L. NARICI AND E. BECKENSTEIN, *Topological vector spaces*, CRC Press, 2010.
- [22] W. K. NEWHEY AND K. D. WEST, *Hypothesis testing with efficient method of moments estimation*, International Economic Review, (1987), pp. 777–787.
- [23] S. R. PARK, S. KOLOURI, S. KUNDU, AND G. K. ROHDE, *The cumulative distribution transform and linear pattern classification*, Applied and Computational Harmonic Analysis, 45 (2018), pp. 616 – 641.
- [24] G. PEYRÉ, *The Numerical Tours of Signal Processing - Advanced Computational Signal and Image Processing*, IEEE Computing in Science and Engineering, 13 (2011), pp. 94–97.
- [25] G. PEYRÉ AND M. CUTURI, *Computational optimal transport*, Foundations and Trends® in Machine Learning, 11 (2019), pp. 355–607.
- [26] Y. RUBNER, C. TOMASI, AND L. J. GUIBAS, *The earth mover’s distance as a metric for image retrieval*, International journal of computer vision, 40 (2000), pp. 99–121.
- [27] S. SHIRDHONKAR AND D. W. JACOBS, *Approximate earth mover’s distance in linear time*, in 2008 IEEE Conference on Computer Vision and Pattern Recognition, IEEE, 2008, pp. 1–8.

- [28] J. SOLOMON, R. RUSTAMOV, L. GUIBAS, AND A. BUTSCHER, *Wasserstein propagation for semi-supervised learning*, in International Conference on Machine Learning, 2014, pp. 306–314.
- [29] C. VILLANI, *Optimal Transport*, Springer Berlin Heidelberg, 2009.
- [30] W. WANG, D. SLEPČEV, S. BASU, J. A. OZOLEK, AND G. K. ROHDE, *A linear optimal transportation framework for quantifying and visualizing variations in sets of images*, Int J Comput Vis, 101 (2013), pp. 254–269.
- [31] Y. ZHANG, R. JIN, AND Z.-H. ZHOU, *Understanding bag-of-words model: a statistical framework*, International Journal of Machine Learning and Cybernetics, 1 (2010), pp. 43–52.
- [32] J. ZHAO, A. JAFFE, H. LI, O. LINDENBAUM, X. CHENG, R. FLAVELL, AND Y. KLUGER, *Detecting regions of differential abundance between scrna-seq datasets*. <https://www.biorxiv.org/content/10.1101/711929v1>, 2019.